Reaction Mechanisms of Mononuclear Non-Heme Iron Oxygenases

Mahdi M. Abu-Omar,* Aristobulo Loaiza, and Nikos Hontzeas

Department of Chemistry, Purdue University, 560 Oval Drive, West Lafayette, Indiana 47907

Received September 21, 2004

Contents

1. Introduction

Aerobic life on our planet relies on the use of molecular oxygen for energy as well as for biosynthesis of important biological compounds in metabolic pathways. Thermodynamically reactions of organic molecules with O_2 are highly favorable with release of a significant amount of energy. However, due to the spin mismatch between ground-state oxygen (triplet) and most organic substrates (singlet), the kinetic reactivity of $^3O_2$ is sluggish. This fact serves an important role in protecting organisms from burning up in air. In a clever design, nature has evolved enzymes to activate molecular oxygen ($^3O_2$) for selective and desirable oxidation processes, overcoming deleterious reactions of O_2 that would lead to oxidative damage. Because transition metals are capable of overcoming the kinetic barriers imposed by spin restrictions,[1] it is not surprising that most oxygen activating enzymes are metalloenzymes.

The different general classes of biochemical reactions with oxygen or its derivatives (superoxide and hydrogen peroxide) that involve metalloproteins are summarized in Table 1. The four-electron reduction of dioxygen to water represents the major source of energy for aerobic organisms.[2] Monooxygenases are distinguished from dioxygenases in that a single oxygen atom is utilized in the product while both oxygen atoms end up in the product of dioxygenases. Exceptions are oxygenases that utilize a specific cofactor (or a second substrate, designated in Table 1 as R′H), which is also hydroxylated. We favor the classification of these as intermolecular dioxygenases to distinguish them from both monooxygenases and intramolecular dioxygenases. The latter class utilizes only one substrate in addition to oxygen, and hence both oxygen atoms from O_2 are incorporated into one product. From a mechanistic standpoint, however, not all hydroxylases operate via activation of dioxygen. Some such as lipoxygenases and intradiol dioxygenases activate the substrate toward attack by triplet oxygen. The relationship between the choice of metal ligands and mode of enzymatic activation (oxygen versus substrate) will be highlighted throughout this review.

Because iron is the fourth most abundant element in the earth's crust, it is not surprising that most hydroxylases are iron dependent. The use of iron was known to ancient civilizations, and its benefits are even singled out in a major scripture: "...And we sent down the iron, wherein there is strength, and many benefits for the people." [Quran 57:25][3]

While much attention has been given in recent years to studying heme enzymes that activate dioxygen (cytochrome P450 and cytochrome *c* oxidase, for example),[4,5] a large number of non-heme iron enzymes are known to catalyze a wide range of reactions with molecular oxygen. Several reviews on mononuclear non-heme iron enzymes have appeared in the literature recently, focusing on structures,[6] spectroscopic and computational methods,[7,8] physical methods, and biomimetic modeling.[9] In this review, we present and analyze results obtained in the past 6 years from primary sequences, structure−function relationships, and chemical kinetics and mechanisms, dealing with mononuclear non-heme iron inter- and intramolecular dioxygenases. The review is divided into three sections with a major focus on the pterin-dependent aromatic amino acid hydroxylases, followed by comparisons with other three substrate hydroxylases, and ending with a discussion of intramolecular dioxygenases. Comments are added wherever appropriate to tie in and emphasize mecha-

* To whom correspondence should be addressed. Phone: (765) 494-5302. Fax: (765) 494-0239. E-mail: mabuomar@purdue.edu.

10.1021/cr040653o CCC: $53.50
Published on Web 00/00/0000 PAGE EST: 25.1

Mahdi M. Abu-Omar was born in 1970 in Jerusalem. He moved to the United States of America in 1988 following the completion of his secondary education and became a U.S. citizen in 1999. He received a B.S. degree (summa cum laude) in chemistry from Hampden-Sydney College, Virginia, in 1992, and pursued graduate studies at Iowa State University of Science and Technology with Professor James H. Espenson (Ph.D., 1996). Following an NIH postdoctoral fellowship with Professor Harry B. Gray at Caltech, he joined the faculty of the University of California, Los Angeles. In 2003, he moved to Purdue University, where he is currently an Associate Professor of Chemistry. His research interests are in the areas of catalytic and bioinorganic chemistry with a focus on studying reaction kinetics and mechanisms, developing structure–function correlations, and designing catalysts that activate inert chemical bonds under mild conditions.

Aristobulo Loaiza was born in Cali, Colombia, and moved to the U.S. in 1979 at the age of six. He obtained his B.S. in biochemistry with honors from California State University, Los Angeles, in 2000. He obtained his M.S. in biochemistry and molecular biology from the University of California, Los Angeles, in 2003. He is currently pursuing his Ph.D. in bioinorganic chemistry at Purdue University.

nistic information that is pertinent to the enzyme's function and selectivity. An attempt was made to be comprehensive; thus, any omission is entirely the fault of the authors and is inadvertent.

2. Aromatic Amino Acid Hydroxylases: Pterin-Dependent Enzymes

Oxidation of an aromatic ring is of importance in both chemistry and biology. In addition to cytochrome P-450,[4,10] flavoprotein hydroxylases,[11a] toluene monooxygenase,[11b] and phenol hydroxylases[11c] that catalyze the oxidation of aromatic substrates, a family of pterin-dependent intermolecular dioxygenases is known to catalyze the hydroxylation of aromatic rings of amino acids. This small group of enzymes includes phenylalanine hydroxylase (PAH), tyrosine hydroxylase (TH), and tryptophan hydroxylase (TPH). The three closely related enzymes are known as the aromatic amino acid hydroxylases (AAAHs). In contrast to flavoproteins, the reduced tetrahydropterin (PH_4) cofactor is not tightly bound to the active site and is allowed to bind and dissociate like a substrate. Phenylalanine hydroxylase catalyzes the rate-determining step in the catabolism of phenylalanine, that is, the hydroxylation of phenylalanine to tyrosine (Scheme 1). Tyrosine hydroxylase catalyzes the oxi-

Nikos Hontzeas was born in 1974 in Athens but has lived most of his life in Canada. He received a B.S. degree in microbiology and immunology from McGill University in 1996, and M.Sc. from the University of Guelph in 1999. In 2004, he completed his Ph.D. studies with Professor Bernard Glick at the University of Waterloo. He was awarded an NSERC graduate scholarship in 2001 and several graduate students awards from the University of Waterloo. He is currently a postdoctoral fellow with Professor Abu-Omar at Purdue University.

Table 1. Summary of Metalloenzymatic Reactions with Dioxygen Species (O_2, $O_2^{\bullet-}$, and H_2O_2)

class	function
transport	$M + O_2 \rightleftarrows M(O_2)$ or $M(O)_2$
oxidase	$O_2 + 4e^- + 4H^+ \rightarrow 2H_2O$
superoxide dismutase (SOD)	$2O_2^{\bullet-} + 2H^+ \rightarrow H_2O_2 + O_2$
peroxidase	$H_2O_2 + RH \rightarrow R(OH) + H_2O$
catalase	$2H_2O_2 \rightarrow O_2 + 2H_2O$
monooxygenase	$O_2 + RH + 2e^- + 2H^+ \rightarrow R(OH) + H_2O$
dioxygenase	
(a) intramolecular	$O_2 + RH \rightarrow R(OH)_2/R(OOH)$
(b) intermolecular	$O_2 + RH + R'H \rightarrow R(OH) + R'(OH)$

Scheme 1. Reaction of Phenylalanine Hydroxylase

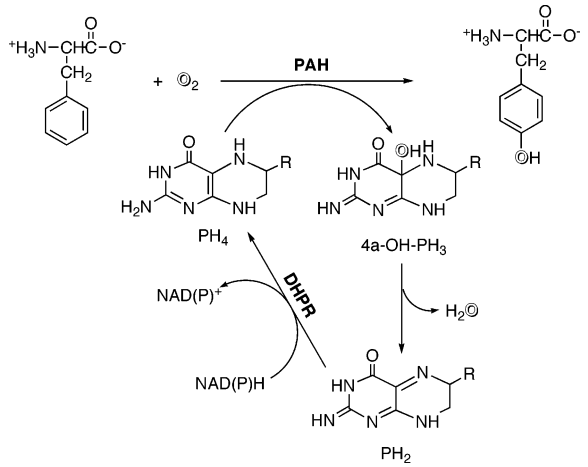

dation of tyrosine to 3,4-dihydroxyphenylalanine (L-Dopa) (eq 1), which is the initial step in the biosynthesis of catecholamine neurotransmitters. Tryptophan hydroxylase catalyzes the formation of 5-hydroxytryptophan (eq 2), a precursor to serotonin. As shown in Scheme 1 and eqs 1 and 2, the initial pterin product from the catalyzed reactions is 4a-hydroxypterin, which dehydrates readily in solution to give the quinonoid dihydropterin.[12−15] The latter is recycled to tetrahydropterin with NAD(P)H by the action of dihydropteridine reductase (DHPR), Scheme 1.[16]

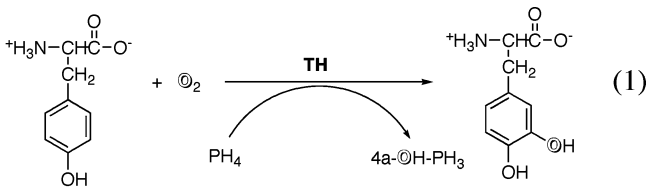

Phenylalanine is present primarily in the liver. Deleterious mutations in PAH resulting in insufficient PAH activity lead to phenylketonuria (PKU), a developmental disorder typified by severe, progressive mental retardation.[17] In PKU patients, phenylalanine accumulates in the blood and starts serving as a substrate for tyrosine amine transfer (TAT) affording the neurotoxin phenylpyruvate (Scheme 2). Tyrosine and tryptophan hydroxylase are found primarily in the central and peripheral nervous system.[18] Dysfunction of these enzymes results in severe neurological and psychological disorders.[19]

Other pterin-dependent oxygenases include anthranilate hydroxylase,[20] mandelate hydroxylase,[21] and glyceryl-ether hydroxylase[22] (eqs 3−5). Unlike most other pterin-dependent enzymes, glyceryl-ether hydroxylase catalyzes aliphatic hydroxylation, as opposed to a more common for this class of enzymes aromatic hydroxylation. Little research and structural studies have been done on these three enzymes, and, therefore, they will not be discussed further. However, the AAAHs are known to share many structural and catalytic properties. They were exhaustively reviewed in 1996,[23] and more specific reviews have appeared subsequently.[24−28] Major advances seen in the past 6 years can be attributed to the availability of high-resolution structures and improvements in recombinant protein expression systems. The latter is key for mechanistic, biophysical, and spectroscopic studies.

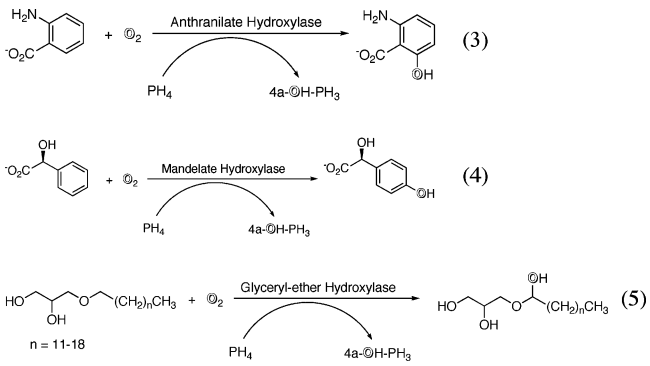

The eukaryotic AAAHs are homotetrameric with each subunit of approximately 52 kDa consisting of three functional domains: an N-terminal regulatory domain, a catalytic domain that contains the active residues and the iron ligands (2 His and 1 Glu), and a C-terminal tetramerization domain.[24] The regulatory domain spans about the first 120 amino acids and the tetramerization domain the last 40 amino acids. PAH forms a dimer when only 13 residues of the tetramerization C-terminal domain are re-

Scheme 2. Normal Metabolic Pathway for Phenylalanine versus PKU Pathway Induced by Malfunction of PAH

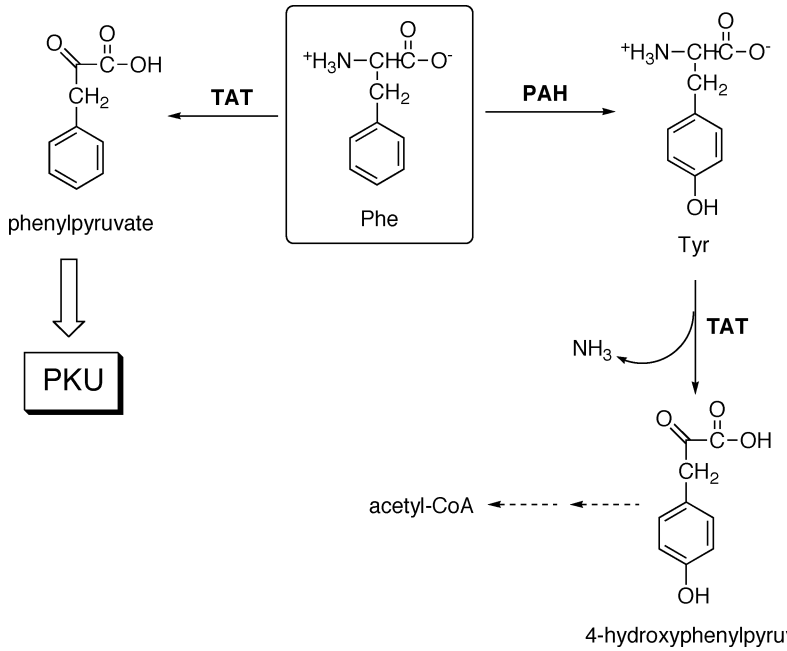

tained.[29] In addition to eukaryotic PAH, several prokaryotic genes have been identified and deposited in the Genbank (vide infra). The structure of bacterial PAH from *Chromobacterium violaceum* has been solved,[30] and the enzyme has been studied in some detail.[31,32] The analogous PAH from *Pseudomonos aeruginosa*, however, has received less attention.[33] In contrast, tyrosine and tryptophan hydroxylase occur only in eukaryotes.

The remainder of this section is broken up into several subareas that detail (1) primary structures, amino acid sequence homology, and evolutionary relationships among the AAAHs; (2) structural comparisons and their relevance to function and stability; (3) regulatory properties; (4) kinetics and mechanisms; and (5) effects of second coordination sphere residues in the active pocket.

2.1. Primary Structures and Evolutionary Relationships

The tetrahydropterin-dependent aromatic amino acid hydroxylases are an example of divergent evolution in which an ancestral gene, possibly prokaryotic PAH, was vertically transferred to eukaryotic cells. PAH has been cloned from both prokaryotes and eukaryotes, whereas TH and TPH seem to be strictly eukaryotic enzymes. Interestingly, to date, there are many amino acid sequences coding eukaryotic PAH that have been deposited on NCBI, whereas there are only about seven prokaryotic sequences. Although the genomes of many bacterial species have been found to include putative PAH genes, in this review we will focus only on published amino acid sequences of PAH, TH, and TPH. In humans and most vertebrates, PAH is present in the liver where it is a necessary enzyme for the catabolism of excess phenylalanine. On the other hand, TH is largely found in the adrenal glands and the central nervous system where it is involved in the biosynthesis of catecholamines, whereas TPH is largely found in the brain and is involved in the biosynthesis of serotonin.

To examine the evolutionary relationships between these three related enzymes, a phylogenetic tree, based on amino acid sequences, was constructed using the Neighbor-Joining method with bootstrap values (Figure 1), and in addition phylogenetic trees were constructed with maximum parsimony. Node support for these trees was evaluated with the bootstrap method and was performed for 1000 replicates. From this tree, it is evident that there are two main clusters, one containing bacterial PAH sequences and the other cluster containing eukaryotic PAH, TH, and TPH sequences. The genetic distances between the bacterial PAH sequences and those of the eukaryotic PAH and TH are similar, indicating that both of these eukaryotic enzymes probably evolved simultaneously from the prokaryotic PAH gene. However, this does not exclude yet another possibility that the prokaryotic PAH and the eukaryotic PAH and TH genes evolved from a common prokaryotic "ancestral" gene independently. The TPH gene, on the other hand, shows the largest genetic distance, indicating that it was most likely the last gene to evolve from either the bacterial PAH or the "ancestral" gene. On the basis of the bootstrap values, it can be concluded that the prokaryotic branch of PAH forms a cluster (bootstrap value of 100) that is divergent from the eukaryotic PAH, TH, and TPH. In eukaryotes, the largest genetic distance is between TPH and TH. The subcluster separating the TPH from the PAH (in eukaryotes) has a lower value (82) than the cluster separating both TPH and PAH from the TH cluster (100).

An alignment of just the eukaryotic hydroxylases shows very high identity in the carboxyl-terminal regions of the proteins of 80%. This strongly conserved part in the amino acid sequences corresponds to the region of the catalytically active 36-kDa proteolytic fragment of phenylalanine hydroxylase.[24] In contrast, at the amino-terminal regions the identity is only about 13%. The sequence heterogeneity observed at the amino-terminal region between the three proteins reflects the different regulatory specificities of the three enzymes (see Regulatory Properties section). When comparing the global alignment of bacterial PAH, eukaryotic PAH, TH, and TPH, there is absolute conservation of a few amino acids. Using the human numbering system for PAH, these residues are Trp187, Ala202, Cys203, Pro225, Gly239, Phe254, Ala259 Phe263, Arg270, Pro281, Asp282, His285, His290, Ala300, Gly307, Leu321, Glu330, Gly332, Gly344, and Tyr386. The importance of these residues cannot be underestimated, because they have been so highly conserved through prokaryotic to eukaryotic evolution. Indeed, many of these residues are absolutely required for activity. For example, the residues His285, His290, and Glu330 are required in the first coordination sphere of the iron, while Phe254 has been implicated in cofactor and substrate binding at the active site of PAH.[29] This strict residue conservation clearly indicates that phenylalanine, tyrosine, and tryptophan hydroxylases stem from a common ancestor, possibly a bacterial PAH gene. However, the amino-terminal sequences constituting the regulatory domains could have been acquired at a later stage in the enzymes' evolutionary divergence or simply had less selective pressure to stay the same.

2.2. Structural Comparisons

The mammalian forms of the AAAHs are structurally and functionally similar. All three, PAH, TH, and TPH, contain oligomerization, regulatory, and catalytic domains. The mammalian AAAHs have 65% sequence identity overall, and 80% sequence identity at the catalytic domain. Unlike the monomeric prokaryotic PAH, the mammalian AAAHs are expressed as dimers or tetramers, which are in equilibrium. Although the last 20 years have produced a plethora of information regarding the hydroxylation mechanism, a detailed hydroxylation mechanism is still elusive. The recent improvements in recombinant DNA technology, which have resulted in better expression of oligomeric proteins, thereby producing larger quantities of biologically active starting material for biophysical studies, have aided our understanding of the molecular events occurring within the active site of AAAHs. Another important tool that has

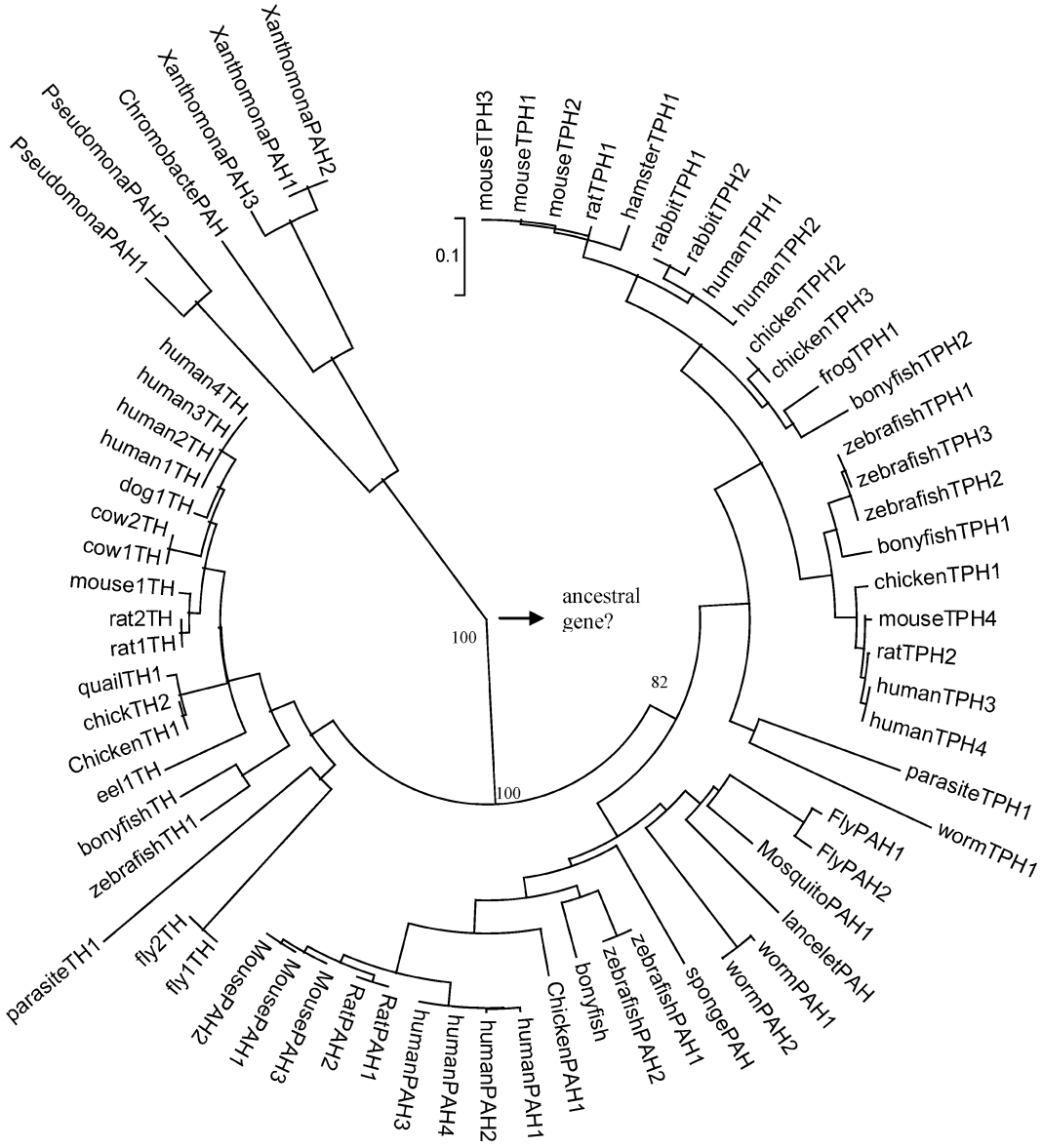

Figure 1. Phylogenetic tree of PAH, TH, and TPH from amino acid sequences available on NCBI.

aided in elucidating the mechanism of mononuclear non-heme iron hydroxylases is the advent of large throughput computers capable of running thousands of structural simulations. We present herein a comprehensive comparison of the available structures for the three AAAHs using data produced over the past 6 years. The data summarized here have shed some light on the interactions between the iron−cofactor, iron−substrate, and the stabilization of the cofactor and substrate at the catalytic core.

Eukaryotic PAH is a 204−217 kDa homotetramer composed of two dimers related by a 2-fold symmetry axis.[34,35] Each monomeric unit is composed of three domains: an N-terminal regulatory domain containing the first 142 amino acids, a 309 amino acid catalytic domain, and a 20−23 amino acid C-terminal domain consisting of two β-strands and a 40 Å long α-helix, which is key in determining the oligomeric state of the enzyme.

Most mammalian PAH structures in the protein data bank are truncated versions of the native form that showcase the catalytic core with particular emphasis on probing the local environment near the non-heme iron center.[35−39] The majority of these structures were cocrystallized with catecholamines bound at the active site, to investigate the mechanism of catecholamine inhibition previously observed for the AAAHs.[23,40] The last 6 years have produced solution (NMR) and solid-state structures of mammalian and bacterial PAH.[30,41,42] Unlike previous structures, the current structures show direct contact between cofactor or substrate and amino acid residues in the first and second coordination sphere of iron, as well as large structural changes associated with substrate binding. Another novel approach in the study of PAH is the use of X-ray absorption spectroscopy to observe substrate/cofactor-induced changes in the active site coordination sphere.[43] Furthermore, molecular docking analysis has corroborated crystallographic results and has shed some light on the molecular basis for catecholamine inhibition.[44]

The catalytic core of all AAAHs contains roughly 220 amino acids of which only 63 are conserved over

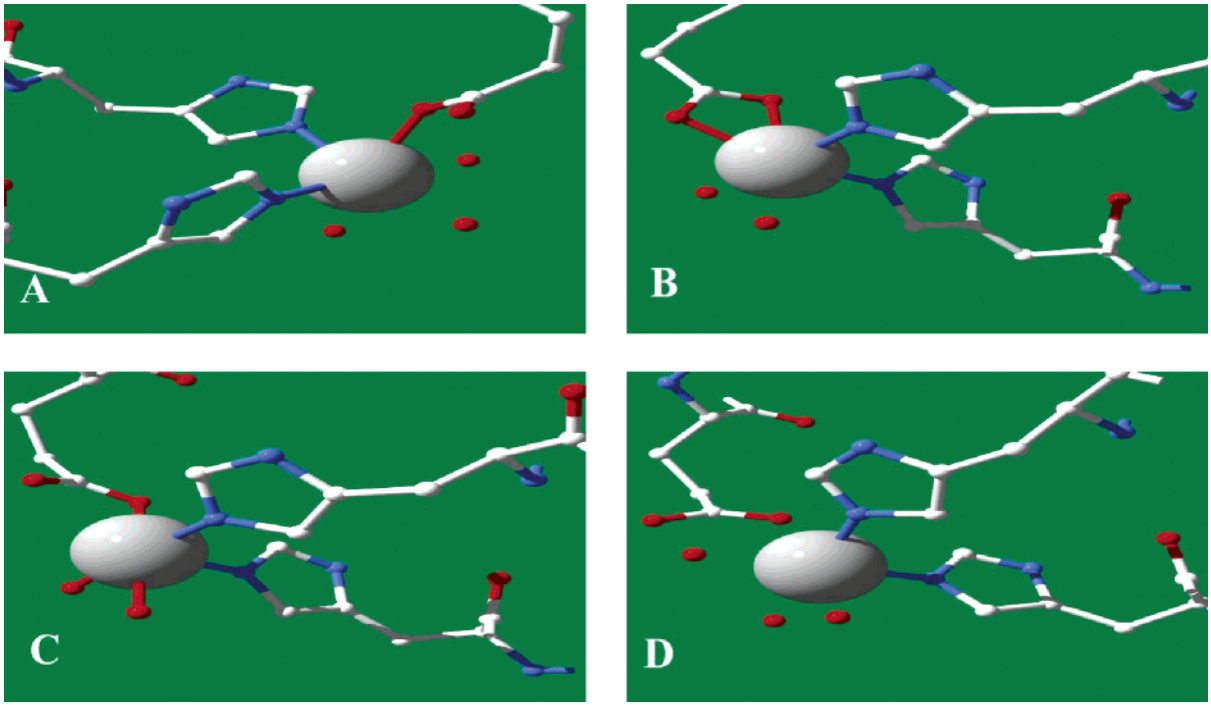

Figure 2. Active sites of (A) hPAH, (B) cPAH, (C) rTH, and (D) hTPH. Non-heme iron atom coordinated in a common 2His-1Glu "facial triad" and water molecules (red spheres in all except TH, where the waters are shown as red cylinders).

hPAH (human), rTH (rat), and cPAH (*Chromobacterium violaceum*). While only 20 (of the 63) catalytic core amino acids are strictly conserved across all known AAAHs, comparison of the catalytic core in cPAH and human PAH shows that both enzymes adopt an α/β fold in a basket-like arrangement despite a modest 35% sequence identity between cPAH and human PAH. The active site of human and *chromobacterium violaceum* PAH has a non-heme iron atom nested in a α-helix "basket-like" groove 13 Å × 13 Å wide and 10 Å deep. The iron atom in hPAH is coordinated to six ligands in an octahedral geometry (Figure 2A).[36] The iron in all AAAHs is solvent exposed, which explains why three of the ligands (in mammalian PAH) are water molecules; the other three ligands are endogeneous residues (His290, His285, and Glu330; hPAH numbering). In human PAH, Glu330 coordinates in a monodentate fashion. In cPAH, however, the iron features a bidentate Glu and two water ligands, maintaining a six-coordinate iron like its human counterpart (Figure 2B). Thus, the bacterial enzyme does differ from the human form in that the equatorial ligand, Glu184, acts as a bidentate ligand leaving only two coordination sites for water ligands instead of three found in the human enzyme (Figure 2).[30]

The hydroxylation of aromatic amino acids is dependent on the binding of the substrates and cofactor at the active site. The binding of cofactor induces conformation changes at the pterin-binding loop (hPAH and cPAH) region, bringing this portion of the enzyme closer to the iron atom. Pterin binding is stabilized by residues in the second coordination sphere (Figure 3). Interactions between cofactor and second coordination sphere residues are observed in the binary complexes of the human (hPAH-Fe(III)·7,8-dihydro-L-biopterin) and the bacterial PAH (cPAH-Fe(III)·7,8-dihydro-L-biopterin). Superposition of the human and bacterial binary complexes shows similar cofactor-binding locations. In hPAH, atoms N2, N1, N8, and O10 on the pterin molecule make important contacts with Gly247, Leu249 (main chain N), Leu249 (main chain carbonyl), and Ala322, respectively.[29] N8 and N3 also interact with two water molecules at the active site. Glu286 in hPAH has been shown to be important in orienting the pterin cofactor.[45] In the binary complex, hPAH-Fe(III)·7,8-dihydro-L-biopterin, Glu286 is positioned 4.4 Å away from the iron and forms a hydrogen bond with one water molecule ligated to the iron and another hydrogen bond with another water molecule that is ligated to N3 of the pterin ring. This type of interaction is conserved in cPAH. In the binary complex, cPAH-Fe(III)·7,8-dihydro-L-biopterin, the corresponding Asp139 makes three contacts with water molecules at the pterin binding site. The water molecules act as bridging molecules that connect Asp139 with the amine moiety, N3 and O4 of the pterin ring. Tyr179 (Tyr325 in hPAH) stabilizes cofactor binding by interacting with a water molecule that is coordinated to pterin. This same interaction is also seen in the human binary complex; in the latter, the water molecule is one of the three iron ligands. Recent kinetic studies have shown that this conserved Tyr is critical for enzymatic activity (vide infra).[46] Both binary complexes show an essential π-stacking interaction between the cofactor and a conserved Phe (Phe107 in cPAH, Phe254 in hPAH). Variations in pterin binding at the pterin-binding loop are a result of inherent amino acid differences in cPAH and hPAH. Another interaction seen in the bacterial binary complex but missing in the human structure is the salt bridge formed by Glu280 and Arg158, which is hypothesized to be critical for stability.

Erlandsen and co-workers were the first to report a structure for an apo AAAH.[30] In addition to apo

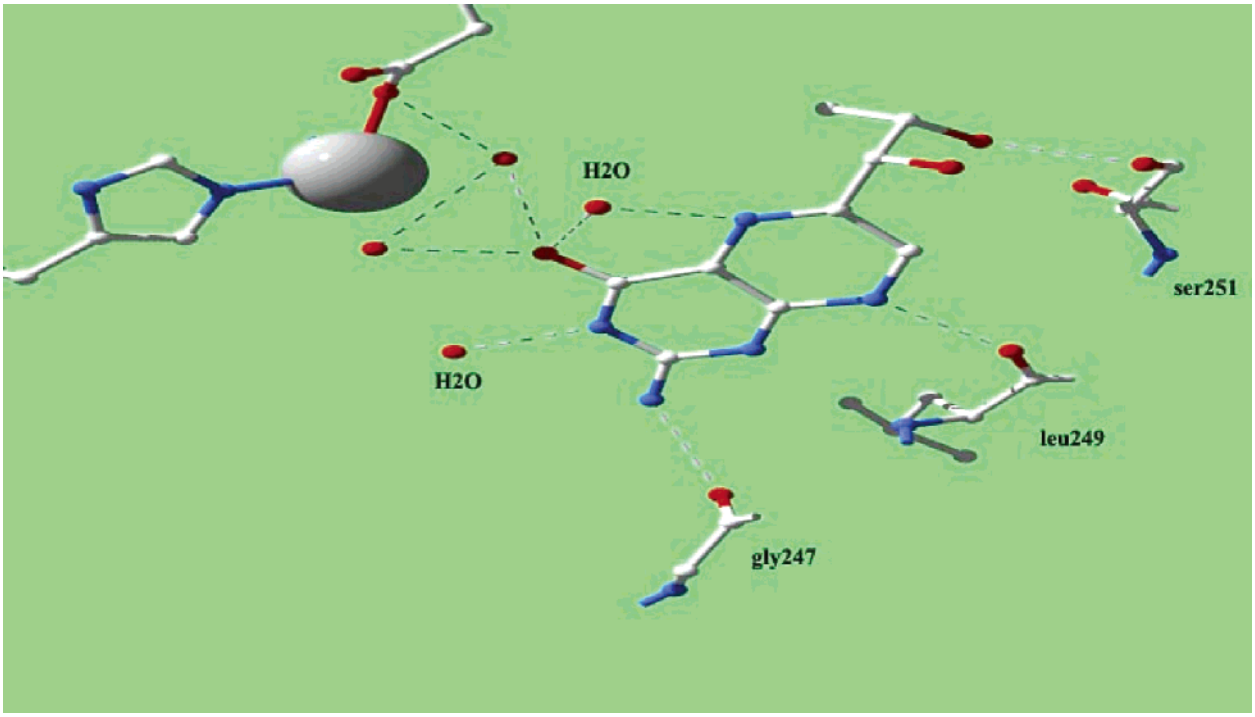

Figure 3. Stabilizing interactions between the pterin cofactor (BH_4) and second coordination sphere residues in human PAH.

cPAH, they also crystallized holo cPAH and holo cPAH with 7,8-dihydro-L-biopterin. Comparison of the apo and metalated structures shows a preformed protein scaffold that only needs minor active-site displacements at Glu184 and His143 to accommodate iron.

A ternary crystal structure of PAH bound to pterin and L-Phe is not available yet mainly due to the disruption of the crystal lattice upon substrate exposure.[41] Nevertheless, Andersen and co-workers have solved the molecular structure of a ternary complex of the catalytic domain of hPAH with tetrahydrobiopterin and substrate analogues 3-(2-thienyl)-L-alanine (THA) and L-norleucine (NLE), which is consistent with the ternary solution structure obtained in the Martinez laboratory by NMR.[41,42,47] Recent structural data support previous results that show the substrate and cofactor bind via an induced fit mechanism evident by the relatively large structural changes observed in the ternary complex PAH-Fe(III)·THA(or NLE)·BH_4. L-Phe binding has been shown to shift the tetramer/dimer equilibrium in the full length enzyme toward the tetrameric form, which suggests that the structural changes observed in the crystal structure are long range and not just limited to the catalytic domain.[48] The binding of L-Phe at the active site changes the coordination of Glu330 to the iron atom from monodentate (before addition of L-Phe) to bidentate. The most significant change is that of Tyr138, which moves from a surface position to a buried position near the active site accounting for a maximum displacement of 20.7 Å. Large structural displacements, however, were not observed in the solution structure. Interactions between the substrate analogue NLE and amino acid residues at the second coordination sphere included hydrogen bonds between NLE and Thr278, Arg270, and Ser349. These interactions are also seen in the solution structure. In addition, two water molecules, in the second coordination sphere, form hydrogen-bond bridges with substrate and Gly346, Glu353, and Tyr277. The structures reported by Andersen are ambiguous about the fate of the three water molecules that coordinate to the iron. X-ray absorption spectroscopic investigations of wild-type hPAH bound to L-Phe and the cofactor analogue 5-deaza-6-methyltetrahydropterin (5-deaza-6-MPH_4), carried out by Wasinger and colleagues, resolve this ambiguity by showing a coordination change at the Fe(II) site.[43] The iron is converted from a six-coordinate distorted octahedral geometry to a five-coordinate square pyramidal structure upon incorporation of the substrate. The change in coordination number has been attributed to the displacement of a water ligand.

Tyrosine hydroxylase (TH) is expressed in mammalian tissues as a tetramer. Crystal structures of the enzyme's catalytic domain, with and without cofactor, are available. Consistent with other eukaryotic AAAHs, each monomer is characterized by an N-terminal regulatory domain, a catalytic core, and a small tetramerization domain at the C-termini. Goodwill and co-workers have solved the crystal structure of the catalytic core and tetramerization domains of rat TH with the cofactor analogue 7,8-dihydrobiopterin (BH_2) bound at the active site.[49] Their structure is the first to show a close interaction between pterin and iron at the active site. At 2.3 Å of resolution, the rat TH catalytic core is structurally homologous to hPAH. Differences in substrate recognition between TH and PAH have been attributed to relative changes in amino acid composition at positions 264, 277, and 379 of hPAH.[50] The crystal structure of rat TH is a truncated form comprised of the catalytic core in a basket-like arrangement of

helices and loops, and a tetramerization domain composed of two short β-strands that connect to a 40 Å long α-helix. In rTH, the iron atom is nested in a 17 Å cleft lined mostly by aliphatic residues. Found exactly 10 Å within the active site nest, the iron coordinates in a square pyramidal geometry with four equatorial ligands (His336, Glu376, and two waters) and one axial ligand (His331) (Figure 2C). Human PAH, in contrast, contains three waters coordinated to the iron. It was hypothesized that the third water in rTH is blocked off by the positioning of Glu376. The active site cleft is lined with mostly hydrophobic amino acid residues that are conserved across all AAAHs. Of specific interest are Phe300, Phe 309, and Pro327, which have been shown to play an important role in pterin-binding. Site-directed mutagenesis analysis of Phe300 and Phe309 revealed that these residues are important for enzymatic activity. Their substitution resulted in a decrease in the production of L-DOPA.[51] Similar to Phe254 in hPAH, Phe300 (in rat TH) also forms π-stacking interactions with the two heterocyclic cofactor rings. The pterin and Phe benzene rings are about 3.5 Å apart and 10° from being parallel. The crystal structure of the binary complex rTH-Fe(III)·7,8BH_2 shows hydrogen bonding between ring atoms in the pterin analogue and active site residues. Leu295, Glu376, and Tyr371 are all within 3.3 Å of the pterin analogue heterocyclic rings and bond to N8, and C4 carbonyl, respectively. The C4 carbonyl is involved in two H-bonding interactions. The first is with the iron ligand Glu376, and the second is with Tyr371. The hydroxyl groups on the tail of the pterin analogue are involved in three additional hydrogen bonds with the main chain amides of Leu294 and Leu295 and a water molecule.

Although a crystal structure of a ternary complex TH-Fe·BH_4·L-Tyr is still unavailable, mutagenesis studies have exposed active site residues that are important for L-Tyr binding.[50,52] Glu326, Glu332, and Asp328 are located within the hydrophobic active site cleft. Site-specific mutagenesis of these residues resulted in an increase in K_{Tyr} of up to 400-fold.

Tryptophan hydroxylase (TPH) is expressed in low quantities in the neurons; recombinant expression of the enzyme in prokaryotic and eukaryotic organisms has been extremely challenging as the recombinant form of the enzyme is expressed as insoluble inclusion bodies, making it difficult to obtain enough starting material for crystallization. Prior to the elucidation of the crystal structure, information about TPH was obtained mainly from mutagenesis studies, kinetic characterization of substrate and cofactor analogues, NMR spectroscopy, and homology-based molecular modeling.[53,54] In 2002, Wang and co-workers were able to obtain the first crystal structure of a doubly truncated version of human TPH with oxidized cofactor 7,8-BH_2 and ferric iron at a resolution of 1.7 Å.[55] The overall structure of the monomeric TPH is very similar to PAH and TH, and the catalytic core was also very consistent with those of PAH, TH, and *Chromobacterium violaceum* PAH. The active site of hTPH is nearly 9 Å deep and 10 Å wide, slightly smaller than that of human and rat TH.[29,49] Directly adjacent to the active site is a 12 Å long and 7 Å deep channel believed to be the binding site of L-Trp.[54] The active site channel is lined by two loops. Similar portal-like loops are also seen in TH, although the conformations of these loop regions vary among the three AAAHs. At the active site, we see the usual ligands bound to the iron atom (Figure 2D). The six-coordinate iron adopts an octahedral geometry, as in hPAH, with three ligands coming from the active site residues (His272, His277, and Glu317) and the other three coming from water molecules.

Pterin binding in hTPH has been studied by NMR spectroscopy using different pterin analogues.[54,56] Crystallographic studies of holo hTPH show that, although the oxidized cofactor 7,8-BH_2 binds in the same position and with similar orientation as in hPAH, different interactions between pterin and second coordination sphere residues have been noted for hTPH. One difference is that the pterin ring is sandwiched between Tyr235 and Phe241 forming π-stacking interactions. Interactions between pterin and Tyr235/Phe241 were corroborated by NMR.[54] Mutagenesis of the Tyr235 results in reduced catalytic activity and an increase in K_{Trp} and K_{BH4}.[53] Aside from the π-stacking interactions, the oxidized cofactor hydrogen bonds to the backbone carbonyl of Gly234 and Leu236. There are additional hydrogen bonds formed between the backbone amide of Leu236 and N1 of BH_2. The pterin O4 atom makes two hydrogen bonds with two iron-liganded water molecules. Furthermore, the carboxylate oxygen atoms in Glu273 form a hydrogen bond to two bridging water molecules that bind the NH2 and O4 regions of the pterin ring, while another water molecule hydrogen bonds to the N3 atom of the pterin ring. Another sequence variation between hPAH and hTPH is Pro238. The corresponding residue in hPAH is Ser251, which hydrogen bonds to the dihydroxypropyl chain of BH_4. In hTPH, Pro238 does not form the same interaction, which would result in a change in conformation of the dihydroxypropyl chain. In hTPH, a water molecule and the backbone carbonyl of Ala309 hydrogen bond to the dihydroxypropyl groups of BH_4.

A partial solution structure of hTPH bound to L-Trp and BH_2 has been solved by Mckinney and coworkers.[54] The structure was docked in to the modeled 3D structure of TPH. The resulting ternary structure TPH-Fe(III)·BH_2·L-Trp resembles that of PAH-Fe(III)·BH_2·L-Phe. The model shows that L-Trp and BH_2 recognition may be influenced by nonconserved amino acids Phe313, Tyr235, and Pro238. Furthermore, the docked structure shows the amino and carboxyl moieties of L-Trp hydrogen bonding to Ser336 and Arg257, while the indole side chain lies in close proximity to Phe313 and Phe318 and π-stacks with His272. Mutagenesis analysis has revealed the importance of Phe313, Arg257, and Ser336 in substrate recognition, binding, and structural stability.[57−60] Phe313, which interacts with L-Trp through π-stacking interactions, corresponds to Trp326 in PAH. Site-directed mutagenesis or "conservative replacement" at these two positions (W326F in hPAH and F313W in hTPH) affected substrate recognition by increasing the relative affinities for L-Trp in PAH and for L-Phe in TPH.

2.3. Regulatory Properties

Structural analysis of multidomain AAAH reveals that the enzymes share structural features including the N-terminal regulatory domain, catalytic core, and C-terminal tetramerization domain. The catalytic core is highly homologous in all three hydroxylases, while the regulatory region seems to be the least homologous domain. The differences in sequence homology at the N-terminus lead to differences in modes of regulation for each of the AAAHs.

The conversion of L-Phe to L-Tyr by phenylalanine hydroxylase is regulated by cofactor inhibition, substrate incubation, and phosphorylation of Ser16 (for review of work done prior to 1998, see refs 23−25). Native holo PAH (with or without BH_4 cofactor bound) is converted from a relatively inactive form (T state) to an active form (R state) upon L-Phe binding at an unidentified site in the regulatory domain. Furthermore, incorporation of L-Phe to the binary complex PAH-Fe(II)·BH_4 results in sigmoidal kinetics. Pretreatment of PAH with L-Phe and/or lysolecithin prior to catalysis stimulates catalytic activity and abolishes the lag portion of the kinetic curve, but incubation of PAH with pterin or pterin analogues prolongs the lag period associated with L-Tyr formation. Phosphorylation of Ser16 by cAMP-dependent protein kinase A (PKA) or calmodulin-dependent protein kinase (CaM-PK) results in up to 4-fold catalytic enhancement and decreases K_{Phe} at the regulatory site. Phosphorylation causes an increase in total protein volume, which is believed to facilitate L-Phe binding at the regulatory domain. Consistent with its inhibitory effects, pterin-incubated PAH is resistant to phosphorylation. A model for the regulatory mechanism of PAH has been proposed (Scheme 3). The following account is focused on the regulatory properties of PAH, TPH, and TH and contains results from work done after 1998.

Scheme 3. Proposed Regulation of Eukaryotic PAH

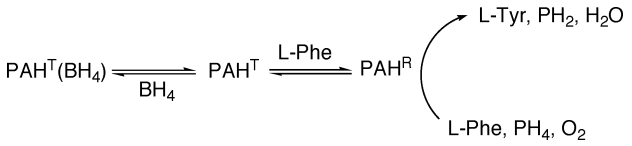

Crystallography and NMR have provided important information that related structure to function, including the elucidation of putative targets for regulation. Unfortunately, most of these structures lack the N-terminal regulatory domain. Chehin and co-workers used spectroscopy to measure the effects of activation by L-Phe, and phosphorylation on full-length holo PAH, with an intact N-terminus. They found global structural changes upon activation of human PAH by its substrate. Furthermore, phosphorylation-mediated activation was shown to cause changes in secondary structure.[61] More recently, surface plasmon resonance (SPR) and intrinsic fluorescence spectroscopy were used for real time monitoring of global conformational changes associated with the L-Phe-induced R-state transition in PAH.[62,63] Furthermore, global conformational changes associated with substrate/cofactor binding have been characterized by limited proteolysis DSC and far-UV CD.[64] Analysis of the effects of L-Phe on DSC thermograms for hPAH suggests that, contrary to previous observations, there are no substrate binding sites at the regulatory domain. Therefore, PAH activation results from homotropic cooperative binding at the catalytic domain. Thorolfsson and co-workers have identified additional regulatory sites at the catalytic core. Cys237, located at the catalytic domain adjacent to the tetramerization domain, and Arg68, located in a loop that is also in close proximity to the oligomerization domain, were found to affect basal activity and L-Phe affinity.[65]

The inactive (or T-state) conformation of PAH is stabilized by cofactor binding.[24,39] Molecular docking of ternary PAH-Fe(III)·L-Phe·BH_2 complex onto the crystal structure of rat PAH catalytic domain shows that Ser251 and Ala322 establish polar and nonpolar interactions with residues at the regulatory domain of rat PAH. These residues have been shown to bind BH_2 and, therefore, are believed to play a key role in stabilizing the T-state of PAH.[47]

Relative to PAH, the information available on the regulatory properties of TH and TPH is limited and perhaps even more ambiguous. What is certain is that their modes of regulation are different. TH and TPH are not regulated by their substrate, but do exhibit product inhibition and inhibition by catecholamines. Furthermore, there are more targets for phosphorylation in TH, relative to PAH and TPH. Phosphorylation of TPH and TH is enhanced by 14-3-3 protein, a neuronal protein which belongs to a family of peptides involved in signal transduction.[66−68] There are four serines in TH (Ser8, 19, 31, and 40) and two in TPH (Ser58, 260).[53] All of the phosphorylation sites on TH are either phosphorylated by cAMP-dependent kinase A (PKA) and/or calmodulin-dependent protein kinase (CaM-PKII in TH); in addition, Ser31 has been found to be phosphorylated by mitogen-activated protein (MAP) kinase. The kinase responsible for Ser8 phosphorylation remains elusive. Cam-PKII and PKA target Ser 58 and Ser260 of TPH, although the activation is not as pronounced as in TH and PAH.[53] Unlike TH, definitive data show that phosphorylation-dependent activation of TPH takes place at the regulatory site.[69]

Phosphorylation enhances enzymatic activity by increasing the rate of inhibitor dissociation. Ramsey has shown that phosphorylation at Ser40 affects the rate constant for the dissociation of L-DOPA and dopamine in TH as well as for other catechols; the loss in binding affinity after phosphorylation was accredited to a decrease in enthalpy of interaction.[70,71] Recently, two other TH-activating kinases, mitogen and stress activated protein kinase 1 (MSK1) and p38 regulated/activated kinase (PRAK), have been identified.[72] Human TH was phosphorylated by MSK1 and PRAK at Ser40 and Ser19, respectively. Phosphorylation by MSK1 resulted in a decrease in K_M for BH_4 and an increase in V_{max}. On the other hand, phosphorylation by PRAK had no effects on V_{max} and K_M. Binding of 14-3-3 protein was enhanced by phosphorylation, and the presence of this protein inhibited

Table 2. A Sample of Kinetic Constants for a Variety of Aromatic Amino Acid Hydroxylases

	$K_M/\mu M$					
enzyme	BH_4	$6MPH_4$	$DMPH_4$	AA subs.[a]	k_{cat} (V_{max})/s^{-1}	ref
rPAH[b]		61		170	9	83
hPAH[c]	29	88		175[d]	1.2	85
103−424 hPAH[e]	40			91	8	29
cPAH[f]	21	17	44	61[g]	37[g]	32
rTH[h]	18			11	1.5	86
102−416 oTPH[i]	135	177		48[j]	1.1	14
SmTPH[k]	7			22[l]	0.2	81

[a] AA subs. = amino acid substrate (L-phenylalanine for phenylalanine hydroxylase, PAH; L-tyrosine for tyrosine hydroxylase, TH; and L-tryptophan for tryptophan hydroxylase, TPH). [b] Recombinant hepatic rat liver enzyme activated with lysolecithin and L-Phe. [c] Recombinant tetrameric human PAH. [d] With BH_4 as cofactor. [e] Dimeric hPAH missing the regulatory domain. [f] Bacterial PAH from *Chromobacterium violaceum*. [g] With $DMPH_4$ as cofactor. [h] Recombinant rat tyrosine hydroxylase. [i] Monomeric catalytic domain of rabbit TPH. [j] With BH_4 as cofactor. [k] Recombinant TPH from the human parasite *Schistosoma mansoni*. [l] The value reflects $S_{0.5}$ due to substrate inhibition.

dephosphorylation by up to 82%. Phosphorylation of Ser19 enhanced the rate of phosphorylation at Ser40 in vitro and in vivo.[73] Substitution of Ser40 with aliphatic amino acids S40V and S40A results in intermediate levels of activation, but a conservative mutation at this position does alter the degree of activation relative to wild type. Surprisingly, S40E enzyme behaved like the phosphorylated enzyme.[74]

Low sequence homology at the regulatory domain of all three eukaryotic aromatic amino acid hydroxylases has been proposed to be an underlying cause for their different modes of regulation. Information on PAH is more abundant relative to TH and TPH. Regulatory studies on PAH have yet to elucidate the substrate activation site at the regulatory domain. Despite the recent proliferation of structural data, there is still a lot of debate about the exact changes in conformation associated with activation of PAH. Furthermore, regulatory studies of TH were originally difficult to interpret because the expression system yielded inhibitor-bound starting material.[70] Less clear is the mechanism of activation in TPH. Improvements in expression yields of full-length TPH are perhaps the first step in this challenging endeavor.

2.4. Kinetics and Reaction Mechanism(s)

Given the high sequence homology in the catalytic domain of the AAAHs (vide supra) and structural similarity,[24,30] the assumption is made that they all share a common catalytic mechanism. As far as substrate selectivity is concerned, the AAAHs, unlike cytochrome P450 enzymes, are not promiscuous. The active site of the AAAHs features a constricted binding site that does not accommodate just any organic substrate. However, alternate amino acid substrates, mainly substituted aromatic amino acids, are reactive to some extent with each of the AAAHs.[25] Tyrosine hydroxylase is capable of hydroxylating phenylalanine and tryptophan albeit at much slower rates than the native substrate. Phenylalanine hydroxylase can function as a poor tryptophan hydroxylase. In addition to aromatic hydroxylation, PAH has been shown to effect sulfoxidation and epoxidation of L- and D-methionine and [2,5-H_2]phenylalanine, respectively.[33,75] Even though the regulatory domains of eukaryotic AAAHs are divergent and exhibit different mechanisms of regulation/activation (vide supra), they are not responsible for the amino acid (substrate) specificity of these enzymes. Bacterial PAH, which lacks a regulatory domain, and a truncated form of the human enzyme that lacks regulation are still unable to react with tyrosine.[29,30] Recent mutagenesis studies on PAH and TH have identified key amino acids in the active pocket that are potentially responsible for the observed substrate specificity.[50] Thus, the catalytic domain is liable for the absolute substrate specificity in these enzymes. Phosphorylation of the regulatory domains in all three enzymes (PAH, TH, and TPH) and substrate activation by phenylalanine in PAH induce conformational changes that affect accessibility to the active site.[39,62]

The accepted biological pterin cofactor used in the pterin-dependent enzymes is tetrahydro-L-biopterin (BH_4); other synthetic pterins, however, are effective and have been employed in vitro.[25] 6-Methyltetrahydropterin ($6MPH_4$) has been most commonly employed with eukaryotic enzymes, and 6,7-dimethyltetrahydropterin ($DMPH_4$) is most reactive with bacterial PAH from *Chromobacterium violaceum*.[31,32] The pyrazine ring of the pterin is not required for activity; 2,5,6-triamino-4-pyrimidinone, for example, has been employed successfully with PAH.[76] However, the pyrimidine ring is essential for cofactor activity.[77] Reduced pterin is capable of reducing the ferric iron in these enzymes to the active ferrous (Fe^{II}) form.[78] This reduction has been suggested to be relevant in vivo as inevitably some of the enzyme oxidizes to iron(III) and ceases to be a catalyst. However, little is known about the mechanism of the active-site iron reduction by BH_4; kinetics suggests a one-electron process involving a trihydrobiopterin free radical intermediate.[78] In the case of bacterial PAH, dithiothreitol (DTT) can be used to reduce the iron and as sacrificial reductant under steady-state conditions to keep the cofactor pterin reduced so the latter is employed as a cocatalyst.[31,32] In contrast, DTT has been shown to inactivate purified human PAH.[79] The K_M values for pterin (PH_4) are generally in the range of 20−60 μM, for the aromatic amino acid substrates in the range 50−200 μM, and for dioxygen 60−85 μM. Maximal activity (k_{cat}) spans a wide range of <1 to >30 s^{-1}. A sample of K_M and k_{cat} values is provided for each of the AAAHs in Table 2. The reported K_M values for each substrate in Table

2 were obtained at saturating concentrations of the two other substrates. TH and TPH display substrate inhibition as well as feedback product inhibition.[80,81] Mammalian PAH features complex kinetics and cooperative binding due to allosteric activation by the amino acid substrate.[82,83] Recombinant human PAH undergoes nonenzymatic deamidation reactions of labile asparagines. The extent of deamidation depends on the length of induction period during protein overexpression in *E. coli*.[84] Because the deamidations affect the catalytic efficiency of the enzyme and its biophysical properties, it was concluded that the labile amide groups are located in the catalytic domain of hPAH and suggested that the deamidation reactions may play a role in catalytic regulation.

Unambiguous steady-state mechanisms have been assigned to only two enzymes from the AAAHs, rat tyrosine hydroxylase (rTH)[80] and *Chromobacterium violaceum* phenylalanine hydroxylase (cPAH).[32] Both investigations demonstrated a fully ordered ter-bi sequential mechanism. In other words, catalytic chemistry ensues only in the presence of all three substrates (pterin, aromatic amino acid substrate, and dioxygen) in the enzyme's active site. In the case of rTH, the kinetic data were interpreted in favor of pterin binding first, followed by a rapid equilibrium binding of O_2, and tyrosine binding last. This result has implicated potential formation of the hydroxylating species in the absence of substrate, but detection of oxidizing intermediates in frozen enzyme samples has not been observed yet for this family of enzymes. However, the data for the bacterial phenylalanine hydroxylase cPAH were indicative of the following binding order: pterin, phenylalanine, and oxygen. The kinetics on cPAH was also consistent with reversible binding of O_2 as the last substrate. Nevertheless, additional support (spectroscopic or otherwise) for reversible binding of dioxygen is still lacking. Recent high-resolution structures of hPAH with a substrate analogue[41] and spectroscopic studies on the active site iron of rPAH[8] corroborate the binding order elucidated with the bacterial enzyme, as the most significant geometrical changes on the iron (from six- to five-coordinate) occur only in the presence of both the pterin cofactor and the amino acid substrate. The steady-state mechanisms for TH need to be reevaluated given the strong similarities between the enzymes and accumulating evidence in favor of oxygen binding last.

Kinetic analyses have been carried out on rPAH, but these have been less decisive possibly due to complications imposed by both substrate activation and negative cooperativity of the cofactor BH_4.[82] A partial assignment of substrate addition to truncated rabbit tryptophan hydroxylase (oTPH) with BH_4 is consistent with the order observed for bacterial PAH, cofactor first, tryptophan second, and oxygen last.[87]

Even though it is agreed upon for the AAAHs that catalysis does not commence until all three substrates are present in the active site, the exact nature of the rate-determining step and consequent molecular mechanism remain unresolved. It is accepted, however, that formation of the oxidizing intermediate is rate determining, because deuteration of the aromatic ring does not display a discernible kinetic isotope effect. Therefore, substrate oxidation is fast. ^{18}O kinetic isotope effect observed for the second-order rate constant $k_{cat}/K_M(O_2)$ of rTH has been explained in favor of one electron reduction of dioxygen to superoxide as the rate-determining step followed by a fast recombination of superoxide and the pterin radical cation to afford 4a-hydroperoxopterin (pathway A in Scheme 4).[88,89] The latter is reminiscent of the reaction characterized for flavoproteins.[90] The initial formation of pterin hydroperoxide without metal participation suggests that a peroxide shunt, in principle, should be possible with the AAAHs. However, hydrogen peroxide as well as organic hydroperoxides so far has not been successful in effecting aromatic hydroxylations with this family of enzymes and bypassing the pterin requirement. The ^{18}O kinetic isotope effect is also consistent with an equilibrium binding of O_2 to iron(II) and single electron transfer from the dioxygen adduct to pterin (pathway B in Scheme 4).[88]

Recent crystallographic[41] and spectroscopic studies[8] show change in the iron(II) geometry from six- to five-coordinate in PAH upon binding of both pterin and phenylalanine. This observation indicates the presence of an open coordination site to accommodate molecular oxygen given the order of substrate binding under catalytic conditions involves O_2 as the last substrate to bind. Furthermore, kinetic studies on bacterial PAH are in agreement with reversible binding of O_2, which would favor metal site coordination. However, binding of O_2 to a hydrophobic site away from the metal cannot be excluded. Whether the initial steps of O_2 activation involve the metal or not (pathway A versus B in Scheme 4), it is well established that substrate hydroxylation in the AAAHs requires iron. Thus, the metal must be involved in the hydroxylating species and a pterin hydroperoxide by itself is not capable of effecting aromatic oxidation. The agreed upon pathway thus far, which lacks direct experimental support, is the formation of a bridging peroxypterin complex with iron (Scheme 4). This iron(II) peroxypterin complex presumably undergoes heterolytic bond cleavage to afford 4a-hydroxypterin (carbinolamine) and iron(IV) oxo species. The initial formation of 4a-hydroxypterin prior to dehydration has been demonstrated for all three AAAHs.[25,14,91] Furthermore, a point mutant of tyrosine hydroxylase was shown to decouple O−O bond cleavage from tyrosine hydroxylation giving quantitative yields of 4a-hydroxypterin from $6MPH_4$ with reduced levels of dihydroxyphenylalanine.[58] Also, tryptophan hydroxylase with tyrosine as substrate afforded a larger amount of 4a-hydroxpterin than DOPA.[91,92] These results are consistent with oxygen−oxygen cleavage taking place in a separate step from substrate hydroxylation. Enzymatic oxidation by an aromatic amino acid hydroxylase of tetrahydropterin to dihydropterin and hydrogen peroxide (eq 6) is controversial.[25] A metal-independent but substrate (L-Phe)-dependent pterin oxidase activity has been claimed for a bacterial phenylalanine hydroxylase.[31] However, these results have not been

Scheme 4. Reaction Mechanism for Pterin-Dependent Aromatic Amino Acid Hydroxylases[a]

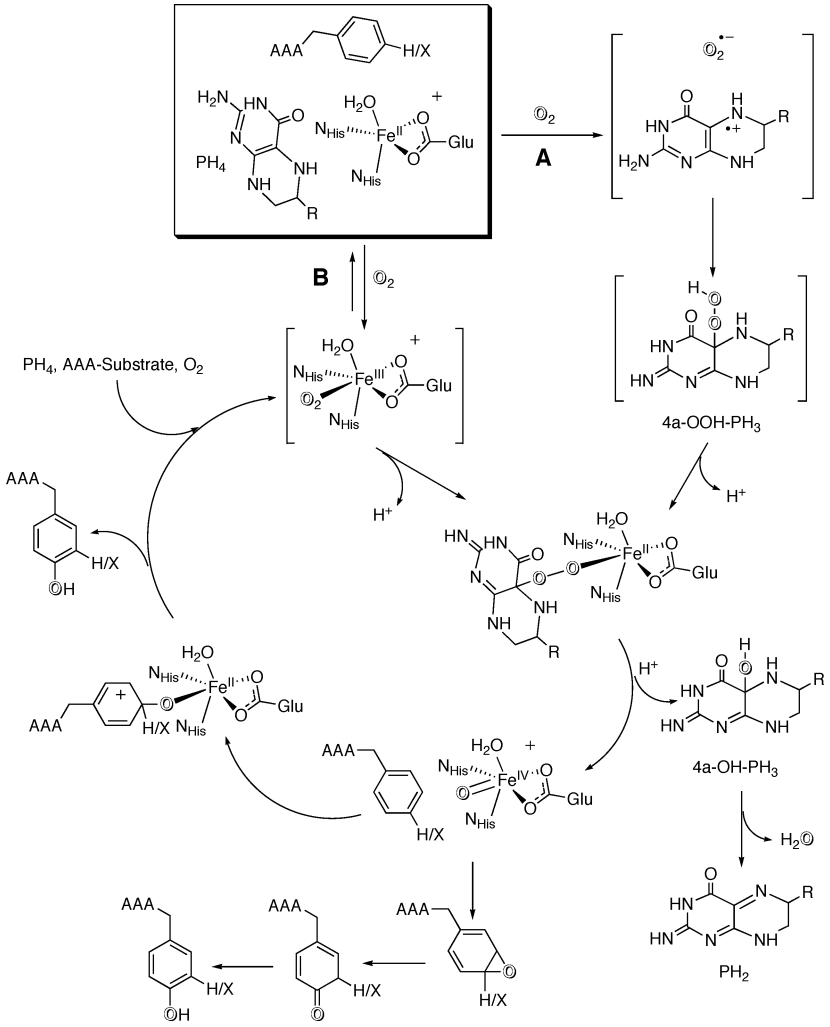

[a] Pathway A denotes iron-independent initial stages of O_2 activation. AAA is short for aromatc amino acid, and X represents isotopically labeled hydrogen (D or T), CH_3, Br, or Cl.

demonstrated for other enzymes in this family, nor were they reproducible.[93]

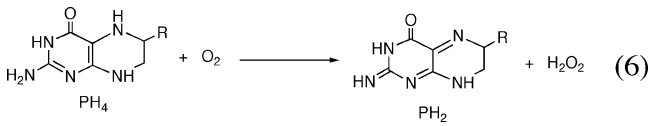

(6)

The proposed chemical mechanism for the AAAHs is distinctly different from the more established mechanism of cytochrome P450 enzymes.[4,94,95] The latter involves Fe^{V}=O (more precisely, Fe^{IV}=O and porphyrin radical cation), which upon reaction with substrate regenerates iron(III). In contrast, the iron(IV) oxo in the AAAHs oxidizes the substrate to restore iron(II), which is ready to react with further oxygen and substrates. The substrate oxidation step in the AAAHs is also distinct from that proposed for P450 enzymes, the "oxygen rebound mechanism."[94] Phenylalanine substrates with para substituents, such as deuterium, chloride, methyl, or bromide, are catalytically converted by PAH to tyrosine products in which the para substituent has migrated to the meta position (Scheme 4).[96] This is known as the "NIH shift" mechanism. To rationalize this observation, which argues against C−H abstraction, aromatic epoxidation has been suggested. A cationic intermediate is another possibility that is consistent with a 1,2-hydrogen shift.[97] Finally, an inverse kinetic isotope effect has been observed for TPH with deuterated substrates.[91] The interpretation thereof was taken in favor of a hybridization change on the terminal oxo of iron, which is uniform with cationic electrophilic substitution. Both possibilities are illustrated in Scheme 4.

2.5. Effects of Second Coordination Sphere Residues

Structural data on the three members of the aromatic amino acid hydroxylases have identified extensive similarities in the overall fold, active site iron, and residues that are critical for cofactor (pterin) recognition.[24,29,41,55] The high level of conservation of these aspects among PAH, TH, and TPH is striking. However, structural data have provided subtle differences in residues of the active pocket (second coordination sphere and beyond) and their potential role in substrate specificity and catalysis. Of course, structural data provide the starting point for hypotheses and speculations of structure−function relationships to be tested experimentally via biochemical techniques. The structures themselves do not provide

Table 3. Kinetic Constants for Mutants that Involve Second Coordination Sphere Residues of the AAAHs

	PH_4[a]		AAA substrate[b]		
enzyme	K_M/mM	V_{max}/s^{-1}	K_M/mM	V_{max}/s^{-1}	ref
wt hPAH[c]	39 (BH_4)	5	91	8	29
E286A hPAH	2000 (BH_4)	0.007	35	0.005	29
E286Q hPAH	53 (BH_4)	0.1	488	0.09	29
F254A hPAH	72 (BH_4)	0.6	600	1.4	29
F254L hPAH	163 (BH_4)	6	53	8	29
wt rTH[d]			109 (L-Phe)	1.6	100
Y371F rTH			10 (L-Phe)	1.4	100
wt cPAH[e]	44 ($DMPH_4$)	36	60	36	46
Y179F cPAH	10 ($DMPH_4$)	2	17	1.3	46
Y179A cPAH	58 ($DMPH_4$)	3	500	3.6	46

[a] The specific pterin cofactor is shown in parentheses next to the K_M value, obtained at saturating concentrations of Phe and O_2. [b] AAA = aromatic amino acid, assumed to be L-Phe for PAH, L-Tyr for TH, and L-Trp for TPH, unless specified otherwise in parentheses next to the K_M value, obtained at saturating concentrations of pterin and O_2. [c] Dimer catalytic domain (residues 103−424) of human PAH. [d] Wild-type rat tyrosine hydroxylase. [e] Wild-type *Chromobacterium violaceum* phenylalanine hydroxylase.

the end answer to mechanistic issues. Of the many active site residues identified by crystallography to be of importance to one extent or another, we will focus on ones that have been characterized in detail and have provided insights on what role certain residues play in defining the enzyme's function.

All three aromatic amino acid hydroxylases feature two imidazole and one carboxylate ligand provided by two histidines and a glutamate residue, respectively. This coordination geometry is ubiquitous, has been noted in many other non-heme oxygenases, and has been coined the name "facial triad" by Que.[98] It has been known that mutation of any of the iron's three ligands to an alanine is not tolerated and yields inactive enzyme that is void of iron. A detailed mutagenesis study has been carried out recently with TH in which each histidine ligand was mutated systematically to glutamate and glutamine, and the glutamate ligand to glutamine and histidine.[99] While some of the mutants retained high affinity to iron binding, none had enzymatic hydroxylase activity. This result demonstrates the "plasticity" of the first coordination shell ligands in these enzymes.[99]

In human PAH, the pterin cofactor interacts through several hydrogen bonds with two water ligands that are coordinated to the iron as well as to the main chain carbonyl oxygens of residues Gly247, Leu249, and Ala322.[29] This hydrogen-bonding network involves Glu286, which is hydrogen bonded to one of the water ligands on iron and via a water molecule to N3 of the pterin cofactor (Figure 3). Phe254 in the so-called second shell of the iron site forms a π-stack with the pterin ring. The point mutants E286A, E286Q, F254A, and F254L have established the role of Glu286 in proper positioning of pterin and of Phe254 in proper substrate binding.[29] The kinetic parameters of these mutants alongside those for wt enzyme are presented in Table 3. Glu286 and Phe254 are highly conserved in the AAAHs.

Another highly conserved residue in the second coordination sphere of catalytic iron is Tyr325 in hPAH, Tyr371 in rTH, and Tyr179 in baterial cPAH. This residue is hydrogen-bonded through its hydroxyl to a water molecule that coordinates to both iron and pterin (Figure 4).[30] A potential catalytic role was initially suggested for this tyrosine.[36] However, the point mutant Y371F rTH displayed activity identical

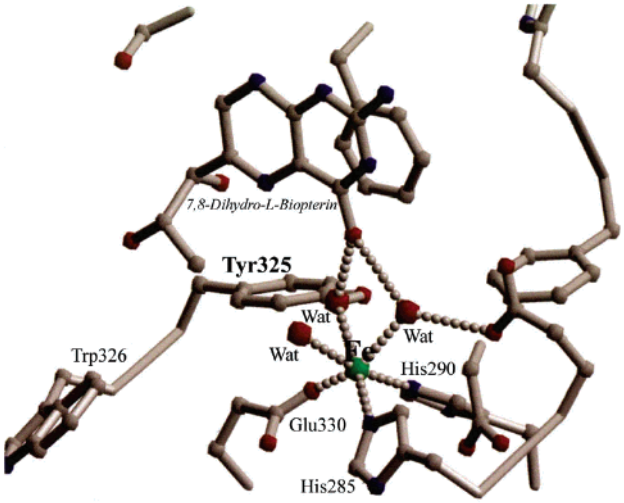

Figure 4. Active site of the binary complex of hPAH with BH_2, highlighting the hydrogen bonding of Tyr325.

to wt rTH, but the mutant showed higher affinity for phenylalanine (Table 3).[100] Thus, its role in the formation of the hydroxylating intermediate was dismissed. Site-specific mutations of Tyr179 in bacterial PAH (Y179F and Y179A) have confirmed a pronounced role of this residue in binding phenylalanine (the substrate) but a secondary effect in the formation of the hydroxylating species.[46] While the point mutant Y179F exhibited higher affinity for phenylalanine, the Y179A mutant displayed a 10-fold increase in K_M(Phe) (Table 3). In contrast, the active site of human PAH is less flexible as the point mutant Y325A has no detectable aromatic hydroxylase activity and forms aggregates instead of the expected tetrameric structure.[101] The latter underscores the importance of Tyr325 in proper folding and function of the enzyme. Interestingly, mutation of Tyr325 in hPAH to Phe affords a fully functional enzyme that, upon further examination by mass spectrometry (MS/MS), demonstrated selective post-translational hydroxylation at residue 325 that restores activity.[101] The rescue of the Tyr325Phe mutant in hPAH via self-hydroxylation presents a novel example of oxidative repair on the molecular level. Other accounts of self-hydroxylation of second coordination sphere residues in non-heme enzymes have been noted to cause inactivation.[102−105]

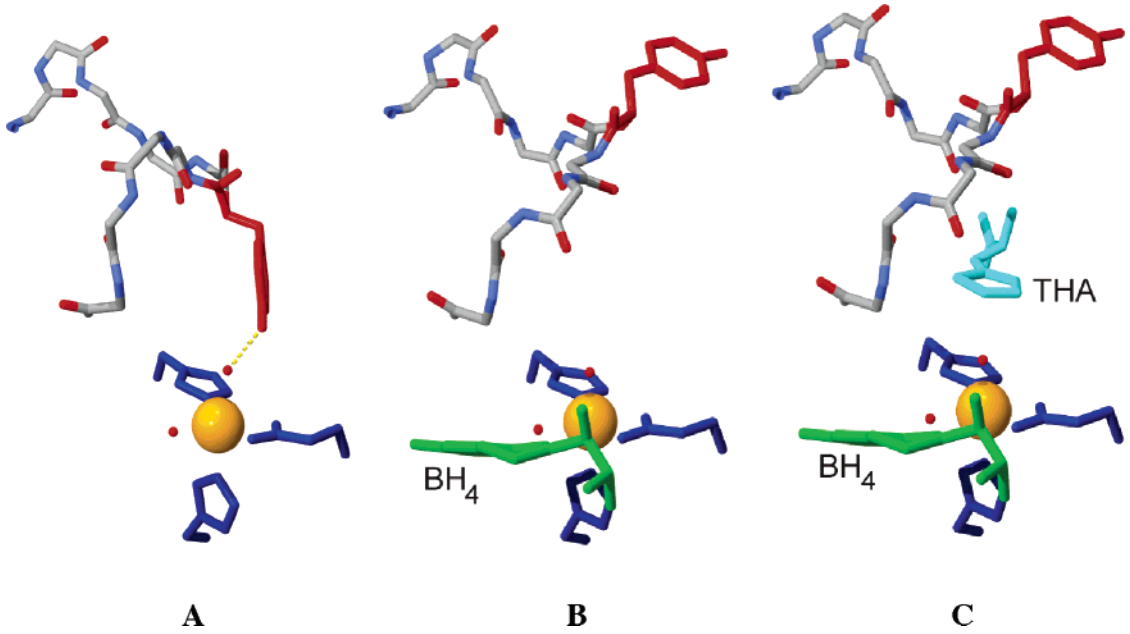

Figure 5. The conformation of loop 125−135 in bacterial cPAH. (A) "Closed" conformation in the absence of any substrates due to hydrogen bonding of Tyr130 to a water ligand on the iron. (B) "Open" conformation as biopterin forms a hydrogen bond with the axial water ligand releasing Tyr130. (C) Modeled binding site of substrate analogue 3-(2-thienyl)-L-alanine (THA) generated from superimposition of the ternary structure of human PAH. Figure created using PDB files 11tv and 1j8t.

Ser395 in the active site of rTH forms a hydrogen bond to the imidazole nitrogen of His331, an axial ligand to the active site iron.[106] This serine residue is conserved in all three members of the AAAHs. The point mutant S395A binds iron and exhibits wild-type activity with both $6MPH_4$ and BH_4.[58] However, the mutant enzyme produces a lower ratio of product (DOPA) per oxidized pterin (4a-hydroxypterin) (DOPA/PH_2 = 0.02) than that observed for wt TH (DOPA/PH_2 = 0.94). This finding demonstrates that, while Ser395 does not affect oxygen−oxygen bond cleavage, it is essential for substrate hydroxylation.

Analysis of the amino acid sequences of PAH and TH was utilized in an elegant mutagenesis study to understand the structural basis of how these two similar enzymes have evolved to discriminate between two very similar substrates.[50] Of the seven residues in the active site of PAH whose side chains are different from those in TH, three residues were identified to be essential for tyrosine hydroxylation, His264, Tyr277, and Val379 (PAH numbering). The TH point mutant D425V (equivalent to residue 379 in PAH, which is a Val) afforded an enzyme with an enhanced affinity for phenylalanine hydroxylation ($(V/K_{Phe})/(V/K_{Tyr})$ = 80 000).[50] In contrast, the PAH point mutant V379D did not exhibit TH activity. However, the double mutation of V379D and H264Q provided a PAH mutant with some tyrosine hydroxylase activity (~1% of that measured for wt TH based on V_{max}). Concurrent with this identification of Asp425 as essential in defining substrate specificity of TH, the recent structure of the catalytic domain of TPH suggested Phe313 and Ile366 in determining substrate specificity.[55] Phe313 and Ile366 superimpose with Trp326 and Val379, respectively, in hPAH, and Trp372 and Asp425, respectively, in TH. ^{1}H NMR study of the ternary TPH·BH_2·Trp structure revealed a ring stacking interaction between Phe313 and the substrate (tryptophan), demonstrating this residue's role in substrate specificity.[54] Furthermore, the W326F PAH mutant increased preference for L-tryptophan, and the F313W TPH mutant showed an enhanced preference for L-phenylalanine.[54] Interestingly, the equivalent mutation of W372F in rTH did not show preference for tryptophan over tyrosine.[107]

The molecular basis for the observed order of dioxygen as the last substrate in cPAH appears to be the change in the iron coordination from six to five, which has been vindicated by the structure of a ternary complex with a substrate analogue.[41] However, the discriminating factor between the binding order of cofactor (PH_4) and substrate (L-Phe) appears to involve a loop in the second coordination sphere of iron, residues 125−135. Careful comparison of the structures of cPAH and its binary adduct with pterin revealed a change in the conformation of this loop from closed to open, as Tyr130 loses its hydrogen bond to a water ligand on the iron (Figure 5A and B).[108] Superimposition of the ternary structure of human PAH suggested that this conformational change is responsible for opening the binding site for phenylalanine (Figure 5C). This mechanism constitutes another example of induced-fit where the binding of the first substrate (pterin cofactor in this case) creates the binding site for the second substrate (L-Phe).[109]

3. Analogous Three Substrate Hydroxylases with Mononuclear Non-Heme Active Sites

3.1. ACC Oxidase: A Key Plant Enzyme

The gaseous hormone ethylene is involved in many plant responses and developmental steps. It is involved in leaf and fruit abscission, seed germination, tissue differentiation, root elongation, formation of

root and shoot primordia, lateral bud development, fruit ripening, production of volatile organic compounds, and the response of plants to biotic and abiotic stresses.[110] Even though ethylene is vital for plant survival, an increased level of ethylene produced in response to various stresses can cause various deleterious symptoms in plants including the onset of senescence and inhibition of root growth.[111] Because 1-aminocyclopropane-1-carboxylic acid (ACC) is the precursor of ethylene, there has been immense interest in agricultural biotechnology to produce transgenic plants with antisense ACC oxidase genes as one way of preventing stress ethylene production.[112] The route to ethylene formation involves methionine conversion to *S*-adenosyl-L-methionine (AdoMet) by the enzyme AdoMet synthetase, and conversion of the latter to 1-aminocyclopropane-1-carboxylic acid (ACC) by the pyridoxal-5-phosphate-dependent enzyme ACC synthase. The final step relies on the iron-dependent enzyme ACC oxidase (ACCO) to produce ethylene from ACC and molecular oxygen (eq 7).

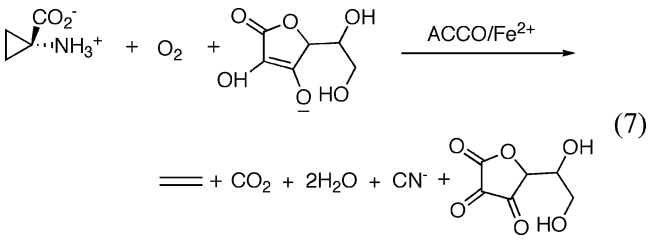

(7)

The isolation of ACC oxidase proved difficult, and it could not be accomplished by conventional biochemical methods. Instead, functional analysis was performed from a cDNA in yeast resulting in the identification of the gene.[112] Based on the similarity of the yeast cDNA to flavanone 3-hydroxylase, ACCO from melon fruits was isolated under conditions that preserved the enzyme's activity, which was observed only after the addition of Fe^{2+} and ascorbate.[113] ACC oxidase is encoded by small gene families.[114] Currently, there are over 197 depositions of amino acid sequences of ACCO on NCBI. All of them are from plants with one that shows ACCO homology from bacterial species (*Rastolnia*). An alignment of many ACCO amino acid sequences shows conservation of a WGFF motif at the amino-terminus of the protein, which could possibly be involved in regulation, as well as an RXS motif, which binds to the terminal carboxylate of 2-oxoglutarate (derived from the structural work on Deacetoxycephalosporin C).

Under normal plant physiological conditions, the enzyme ACCO is abundant, and the rate of ethylene formation is determined by the limiting amount of substrate ACC.[115] However, expression of the ACC oxidase genes has been shown to be differential and affected by many different factors such as ethylene, auxin, developmental and tissue-specific factors, abscisic acid, and brassinosteroids.[116−123] The in vitro activity of ACCO has been shown to be strictly dependent on the exogenous addition of Fe^{2+}, ascorbate, and CO_2 or bicarbonate.[124,125] Initially the mechanism of ACCO was proposed to involve iron-mediated oxygen activation with the reduction of ascorbate producing an iron-bound or diffusible reactive oxygen species (ROS).[126] The reactive oxygen species was proposed to subsequently react with ACC generating a radical intermediate followed by cyclopropyl ring cleavage and ethylene formation.[127−129] Even though the generation of the radical intermediate has been demonstrated, the mechanism has been called into question by recent studies. Currently, there are two competing models for the order of substrate binding, as well as several different suggestions for the roles of bicarbonate, carbon dioxide, and ascorbate.

In the first model, a random binding mechanism has been suggested based on steady-state kinetics and inhibitor studies.[130] Either ACC or ascorbate binds first, dioxygen second, and the remaining species third (ascorbate or ACC). Ascorbate appeared to preferentially bind first. Alternatively, an ordered sequential binding mechanism has been proposed as well based on steady-state kinetics. ACC binds first followed by dioxygen.[131] The binding order of ascorbate could not be clearly distinguished and either precedes ACC binding or follows dioxygen binding. The latter model is supported by previous EPR and ENDOR spectroscopic studies on the nitrosyl adduct of ACCO, wherein ACC was suggested to coordinate to iron in a bidentate fashion, through both the α-amino and the α-carboxylate groups.[132] Furthermore, the spectroscopic results were interpreted in favor of the concurrent binding of ACC and dioxygen onto the iron center. The bidentate coordination of ACC is proposed to lower the redox potential for Fe(II) and prime it for dioxygen binding. This pattern of substrate binding before dioxygen limits oxidative damage to the protein.[131] Recently, under single-turnover conditions, the oxidation of Fe(II) to Fe(III) was noted by the appearance of an EPR-active species.[133] From this observation, a mechanistic pathway involving Fe(III)-peroxo and Fe(IV)-oxo intermediates was postulated.

The role of ascorbate in the production of ethylene remains unresolved. Thrower et al. proposed that ascorbate binds away from the Fe(II) center, to active site residues R244 and S246 (tomato ACCO), which are part of a conserved jelly roll motif.[131] Ascorbate has also been classified as both a cosubstrate[134] and an effector.[133] Furthermore, it was suggested that ascorbate limits small molecule access to iron. In a single-turnover experiment, ascorbate was found to be unnecessary for ethylene production in the presence of bicarbonate. Ascorbate, however, increases dramatically the rate of ethylene production and iron oxidation.[133]

It was suggested that carbon dioxide or bicarbonate functions as an activator.[134] It is unknown whether the activating species is carbon dioxide or bicarbonate, and much remains unresolved about its location of binding. However, it is clear that the presence of carbon dioxide or bicarbonate is essential for proper enzyme function. Rocklin et al. proposed that bicarbonate binds to the conserved arginine and serine active-site residues of a jelly roll motif, while others give evidence for carbon dioxide mediated activation.

Scheme 5. Proposed Mechanism for α-KG-Dependent Enzymes Such as TauD[a]

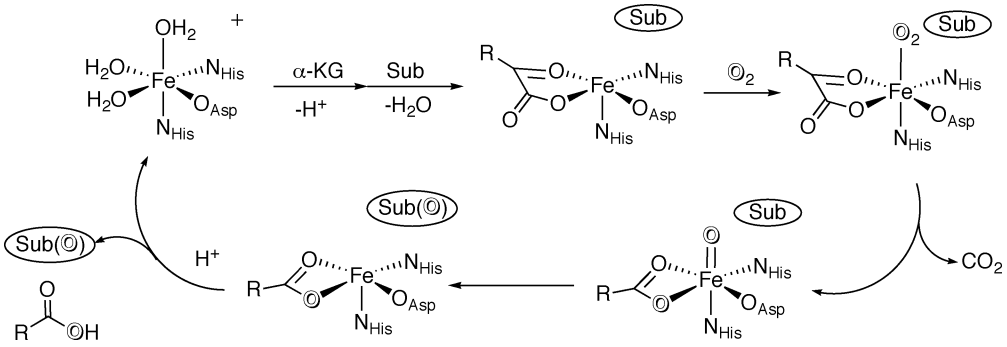

[a] Sub designates substrate.

NIR CD and MCD studies have demonstrated that in the presence of carbon dioxide a five-coordinate distorted square pyramidal geometry for iron is adapted only when both ACC and ascorbate are bound.[134] Carbon dioxide was also found to have a complementary stabilizing role for the ACCO/Fe(II)/ACC distorted octahedral geometry. In the absence of carbon dioxide, 30% of the octahedral complex converts to the square pyramidal form by ACC alone, priming the complex for dioxygen binding, which leads to enzyme deactivation possibly via oxidative damage.

3.2. α-Keto Acid-Dependent Enzymes

One of the most diverse and important groups of mononuclear non-heme iron hydroxylases is the α-keto acid-dependent enzymes. They are ubiquitous and have been isolated from plants, animals, and microorganisms, where they have been shown to participate in a plethora of biological processes ranging from DNA and RNA repair, antibiotic synthesis, to even herbicides. The α-keto acid-dependent enzymes include deacetoxycephalosporin C synthase (DAOCS), 4-hydroxyphenylpyruvate (HPP) dioxygenase, clavaminate synthase (CAS), DNA and RNA repairing *N*-demethylase (AlkB), taurine/2-oxoglutyrate dioxygenase (TauD), asparagines hydroxylase, lysyl hydroxylase, 4-hydroxymandelate synthase, and prolyl-4-hydroxylase. Because an excellent recent review article has covered these enzymes extensively, this section is focused on the recent reports and mechanistic aspects published over the past 2 years.[9a,135]

A consensus mechanism has been proposed for α-keto acid-dependent enzymes (Scheme 5).[7,135,136] The initial state of the enzyme contains Fe(II) coordinated to three water molecules and the 2-His-1-carboxylate "facial triad" motif. Based on steady-state kinetics on various α-keto acid-dependent enzymes, an ordered binding mechanism was concluded in which α-keto carboxylate binds the iron first in a bidentate fashion leading to displacement of two water molecules from the coordination sphere. Subsequently, molecular oxygen binds iron to afford a superoxo Fe(III)-O_2 intermediate, followed by a series of redox reactions with the α-keto acid cofactor. The outcome is CO_2 liberation and formation of the carboxylic acid byproduct concomitant with the generation of Fe(IV) oxo, the proposed hydroxylating species.

In two recent exciting developments, further evidence for the involvement of a high-valent iron oxo intermediate has been presented for the TauD enzyme. The first study employed oxygen-isotope difference resonance Raman spectroscopy, under cryogenic continuous flow conditions.[137] The high-valent iron intermediate featured an absorption maximum near 318 nm, and its resonance Raman spectrum displayed vibrations in the range 750−850 cm^{-1} exhibiting an ($^{16}O/^{18}O$) isotope shift of 26−40 cm^{-1}. Although vibrations near 800 cm^{-1} could be assigned to a peroxo stretching mode (ν_{O-O}), the observed isotopic shifts were not consistent with such an assignment. Thus, the observed peaks at 821 and 787 cm^{-1} were assigned to an iron oxo stretch ($\nu_{Fe=O}$).

In the second investigation, a large kinetic isotope effect ($k_H/k_D \approx 35$) has been measured for the decay of the 318 nm intermediate of TauD. This finding demonstrated the involvement of the 318 nm intermediate in C−H(D) abstraction from taurine (the substrate) and corroborated the assignment of Fe(IV)=O.[138] Direct evidence for the ferryl formulation was provided by freeze-quench X-ray absorption spectroscopy. A tight Fe−O bond length of 1.62 Å was detected, which is consistent with an iron oxygen double bond. This interaction was absent from control samples prepared rigorously in the absence of air. Furthermore, Mössbauer spectra showed that approximately 80% of the iron is in the +4 oxidation state. In comparison, an anaerobic control sample contained no Fe(IV). XANES spectra confirmed a higher oxidation state for the intermediate than the starting complex containing Fe(II). The intermediate, however, had a lower edge energy, which is proposed to represent Fe(IV), but could represent a mixed oxidation state between Fe(III) and Fe(IV). EXAFS oscillations fitted to Fourier-filtered first-shell data and unfiltered data gave the best correlation to a 1.62 ± 0.01 Å Fe−O interaction.

Insight into the iron intermediates involved in catalysis was obtained from a recent study on the alkylsulfatase AtsK, which converts alkyl sulfate esters to aldehyde and sulfate.[139] The molecular structure of AtsK was solved for the apo enzyme, as well as in combination with α-ketoglutarate, α-ketoglutarate and iron, and α-ketoglutarate, iron, and an alkyl sulfate ester needed for catalytic turnover.[139] XANES data, obtained using an AtsK-Fe-αkG binary complex, showed an Fe(III) intermediate bound to histidine and carboxylate ligands. It was also dem-

onstrated that the oxidation of iron(II) bound to the protein is not coupled to the substrate reaction and can occur in the substrate's absence. However, if the iron is oxidized prior to binding to the protein, which is added to an oxygenated protein sample, it does not bind the active site. On the other hand, if iron(II) is added to the protein under anaerobic conditions followed by exposure to oxygen, it remains bound to the enzyme despite its oxidation to Fe(III).

A recent study of the DAOCS enzyme unveiled the formation of an interesting new "booby-trapped" oxidizing intermediate.[140] Using steady-state kinetics, quantum mechanical calculations, and X-ray crystallography, Valegård and co-workers demonstrated that the binding site for the byproduct succinate overlaps with the binding site of the substrate penicillin. Hence, the active oxidizing species is formed prior to substrate binding, but the intermediate is stabilized by the negatively charged succinate, which protects the enzyme from self-hydroxylation. The oxidizing species was proposed to be a planar Fe(II)peroxo because it is less reactive than ferryl and therefore has a longer lifetime. The planar Fe(II)-peroxo intermediate was referred to as a "booby-trapped" oxidizing intermediate. During catalytic turnover, succinate is displaced from the active site and replaced by the substrate penicillin. The loss of the electron donating and negatively charged carboxylate ligand from succinate triggers the reaction of the "booby-trapped" Fe(II)peroxo intermediate with penicillin to give cephalosporin and water.

4. Mononuclear Iron Dioxygenases: Two Substrate Hydroxylases

4.1. Arene *cis*-Dihydroxylation

Rieske dioxygensases are multicomponent enzymes that catalyze the *cis*-dihydroxylation of polyaromatic hydrocarbons with molecular oxygen (eq 8). They are found in soil bacteria, and their reaction constitutes the first step in the biodegradation of aromatic hydrocarbons to *cis*-diols, which are subsequently oxidized by diol-cleaving catechol dioxygenases discussed in the next section. Therefore, Rieske dioxygenases have important applications in bioremediation.[141,142] Aromatic hydrocarbons are recognized as serious environmental pollutants. The enzyme's components are the following: (a) a flavoprotein reductase that contains a Rieske iron−sulfur [2Fe-2S] cluster, (b) a ferredoxin, and (c) an oxygenase component. In addition to the two electrons provided by the substrate, two additional electrons are provided by NAD(P)H via cascades of long-range electron-transfer reactions from the reductase domain to the active site catalytic iron.

(8)

The oxygenase domain of naphthalene 1,2-dioxygenase contains a mononuclear non-heme iron that features two histidine ligands, a bidentate aspartate, and water in its first coordination sphere.[143] It is this

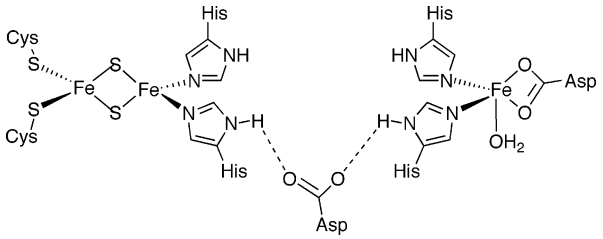

Figure 6. The two metal centers of the oxygenase component of arene *cis*-dihydroxylating oxygenases. The Rieske [2Fe-2S] cluster is linked to the catalytic iron via a hydrogen-bonding network by an aspartate residue in the second shell.

mononuclear site that is believed to be the catalytic site for O_2 activation and subsequent aromatic dihydroxylation. In addition to the catalytic iron, the oxygenase component contains a Rieske iron sulfur cluster [2Fe-2S] with one iron coordinated to two histidines and the other to two cysteines. The Rieske center is connected to the catalytic iron via an aspartate residue that forms hydrogen bonds with histidine ligands on both metal centers (Figure 6). More than three dozen distinct Rieske dioxygneases have been identified. However, among the most studied are naphthalene 1,2-dioxygenase (NDO), phthalate dioxygenase (PDO), anthranilate 1,2-dioxygenase (ADO), and benzoate 1,2-dioxygenase (BZDO). Rieske dioxygenases are versatile enzymes that are capable of carrying out other oxidation reactions besides *cis*-dihydroxylation. These include benzylic oxidation, desaturation, and sulfoxidation.[144−148]

The crystal structure of the oxygenase component of NDO from *Pseudomonas putida* is thus far the only three-dimensional structure available for the oxygenase component of this class enzymes.[149,150] It revealed a mushroom-shaped symmetric $\alpha_3\beta_3$ hexamer.[143,149] The Rieske iron−sulfur cluster and the mononuclear catalytic iron are located within each α subunit, and electron transfer from the [2Fe-2S] cluster to the non-heme catalytic iron site is believed to take place across α-subunit interfaces.[153,154] Structures of the oxygenase domain with bound substrate (naphthalene) or an analogue (indole) are also available, showing the proximity of the substrate from the mononuclear iron site (4 Å).[143] In addition to substrate-bound structures, frozen crystals of the oxygenase of NDO were exposed to O_2 at low temperature and the structures of O_2 adducts of the enzyme were solved.[150] In the absence of substrate as well as in the presence of a substrate analogue, the crystallography studies revealed a side on peroxo ligand with a significant O−O bond elongation (1.4 Å).

Two structures of Rieske dioxygenase reductase component have been solved for phthalate dioxygenase (PDO)[151] and benzoate dioxygenase.[152] The reductase components are homologous to plant-type ferredoxins in the N-terminal region and ferredoxin: NADPH reductases (FNR) in the C-terminal region. The spatial locations of the flavin binding domain and the ferredoxin-like domain are reversed in the two structures.

Recent spectroscopic studies on NDO employed nitric oxide (NO) as a surrogate for O_2 and as means of providing an EPR signal for high-spin Fe^{II}, which

Scheme 6. Proposed Catalytic Cycle for Arene *cis*-Dihydroxylation As Catalyzed by Mononuclear Non-Heme Iron-Dependent Rieske Dioxygenases

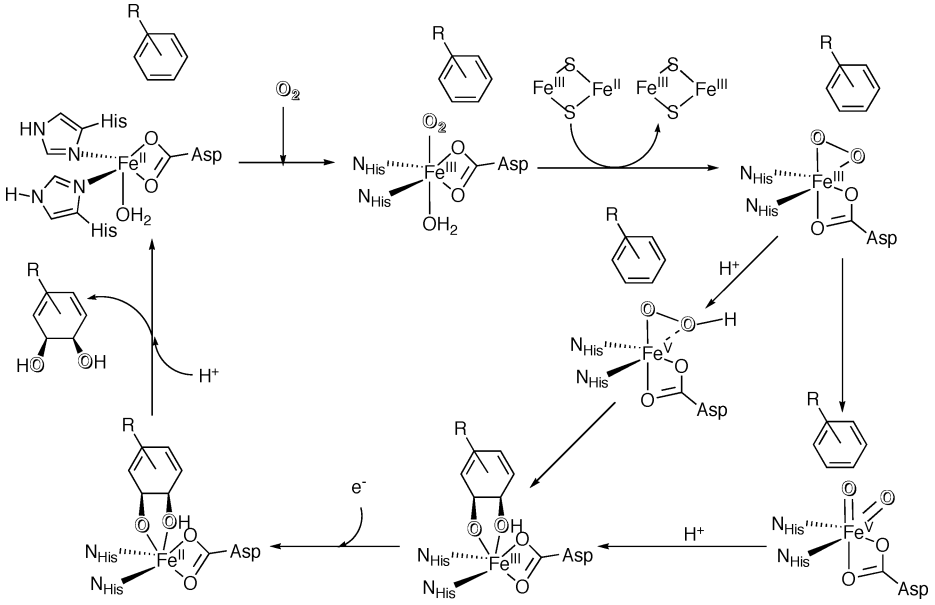

is, otherwise, EPR silent.[155] The effect of substrate binding on the coordination environment of iron and the positioning of the substrate as a function of the oxidation state of the Rieske [2Fe-2S] cluster was probed by high-resolution Q-band pulsed ^{2}H-ENDOR spectroscopy. NO was found to bind with retention of the water ligand, and the positioning of d_8-naphthahlene was found to be dependent on the oxidation state of the Rieske center. The latter suggests that the redox state of the [2Fe-2S] cluster is coupled to the binding site of the substrate. Independent single-turnover kinetics on benzoate dioxygenase has also shown that the rate of electron transfer between the iron−sulfur cluster and the catalytic mononuclear iron is influenced by the substrate, suggesting a new mechanistic role for the substrate in oxygen activation.[156]

Engineered substitution of the bridging aspartate between the two metal centers in NDO (Figure 6) knocked out activity and was interpreted as a result of eliminating the pathway for electron transfer.[157] Substitution of the equivalent aspartate in anthranilate 1,2-dioxygenase with alanine, asparagine, or glutamate resulted in retention of iron binding and the hexameric structure but total loss of activity.[158] The reduction potential of the Rieske center in these point mutants was found to be ~100 mV more negative than the wild-type enzyme. Both the wild-type and the alanine point mutant underwent substrate-dependent oxidation of the Rieske center on the stopped-flow time scale. However, single turnover to give anthranilate dihydroxylation with fully reduced enzyme was observed only with the wild-type enzyme and not the alanine mutant. These results refute the role of aspartate in facile intersite electron transfer or substrate gating and demonstrate the importance of this aspartate in substrate dihydroxylation.

The dihydroxylation reaction in Rieske dioxygenases is believed to take place at the mononuclear catalytic iron site, because reduced iron(II) at that site and a reduced Rieske center ($Fe^{II}Fe^{III}$) provide a competent enzyme for single turnover dihydroxylation reaction.[153,154,156] The accepted mechanism involves reaction of dioxygen with iron to give a side on bound peroxide; the latter has been observed crystallographically.[150] However, the initial stages of the reaction are not fully understood, and the exact structure of the hydroxylating species is also not known. It has been suggested that O_2 binds Fe(II) to give an Fe(III) superoxide adduct in a reversible step.[159,160] Reduction via electron transfer from the Rieske [2Fe-2S] cluster results in the $Fe^{III}(\eta^2\text{-}O_2)$, Scheme 6. The protonation state of the peroxo ligand and whether an iron peroxo complex hydroxylates the arene substrate are among the outstanding mechanistic issues. However, the peroxide shunt, that is, use of H_2O_2 as oxidant in place of oxygen, has been demonstrated successfully for this class of enzymes.[148,161] Also, from a chemical perspective metal peroxo complexes are not known to effect dihydroxylation reactions, but metal oxo species (such as OsO_4) are efficient dihydroxylation reagents for olefins. Therefore, it is possible that the peroxo ligand on iron is cleaved to give high-valent iron oxo, which adds in a [3+2] fashion to the arene double bond. Product dissociation, the rate-determining step under steady-state conditions, occurs upon reduction of the iron site via electron transfer from the enzyme's reductase component via the Rieske center. The affinity of iron(II) for diols is much lower than that of iron(III). The mechanistic possibilities of arene dihydroxylation by Rieske dioxygenases are summarized in Scheme 6.

4.2. Catechol Dioxygenases

Catechol dioxygenases are iron-dependent enzymes ubiquitous to most soil bacteria. They utilize molecular oxygen to cleave the aromatic ring of catechol (dihydroxybenzene) and its derivatives, an important step in the degradation of aromatic compounds particularly polluting haloaromatics.[162−164] Therefore, catechol dioxygenases and microorganisms that can

Scheme 7. Ring Cleavage by (a) Intradiol and (b) Extradiol Dioxygenases To Give *cis,cis*-Muconic Acid and Muconic Semialdehyde, Respectively[a]

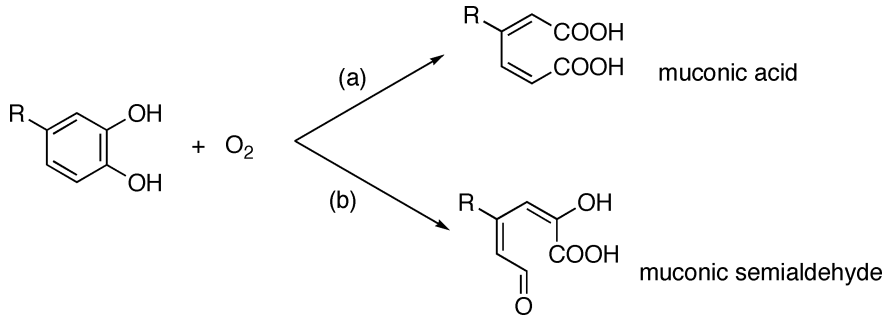

[a] R = H for catechol and R = −COOH, Cl, Br, or F for protocatechuic acid.

utilize haloaromatics as the sole carbon and energy source have attracted attention in areas of bioremediation and environmental microbiology.[165,166] Two classes of catechol dioxygenases have been recognized, and they are distinguished by their regioselectivity in effecting ring cleavage. Intradiol dioxygenases cleave the carbon−carbon bond of the enediol, while extradiol dioxygenases effect the cleavage of the carbon−carbon bond adjacent to the enediol functionality (Scheme 7). The exclusive regioselectivity of each enzyme suggests a distinct mechanism for each. Indeed the coordination environment around the metal active site is quite different for each of the catechol dioxygenases. The intradiol cleaving dioxygenases have an Fe(III) as the active form with trigonal bipyramidal geometry (Figure 7). The ligands are two imidazoles and two phenoxides provided by histidine and tyrosine residues, respectively. The fifth ligand is hydroxide. The active site iron in the intradiol dioxygenases is thus neutral in charge. In contrast, the extradiol dioxygenases have an Fe(II) in the active site with two histidines and a glutamate ligand that form a square pyramidal coordination around the iron with two ligated water molecules (Figure 7). In a few examples, extradiol dioxygenases have been characterized with Mn(II) as the active site metal instead of iron.[167,168]

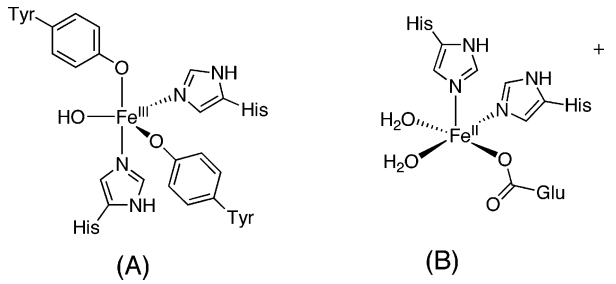

Figure 7. Iron coordination environment in (A) intradiol and (B) extradiol dioxygenases.

Even though intradiol dioxygenases are more studied and thus more understood, extradiol cleavage is more common than intradiol cleavage in biological degradation of aromatic compounds. The difficulty in studying extradiol dioxygenases as compared to intradiol dioxygenases could be attributed to the lack of spectroscopic probes available for Fe(II) versus Fe(III). However, recent crystallographic structures on three different extradiol dioxygenases have provided insight on substrate binding and oxygen activation and confirmed previous spectroscopic studies.[169−174] Structural studies demonstrated that the substrate binds to iron in an asymmetric fashion displacing the two water ligands. This leaves the site trans to the glutamate ligand for binding oxygen. This is supported by the binding of NO, a surrogate of O_2, in that position, and by steady-state kinetics, which showed an ordered binding mechanism with substrate binding prior to O_2.[162] EXAFS studies on the enzyme substrate binary complex have also indicated asymmetric binding of the substrate, which is consistent with the substrate acting as a monoanionic ligand.[175] This mode of catechol binding in extradiol dioxygenases is quite distinct from that observed for the intradiol dioxygenases (vide infra) and is believed to be key in defining the enzyme's regioselectivity.

Despite the fact that little is known about the redox steps following oxygen binding in the extradiol dioxygenses, a mechanism has been proposed (Scheme 8).[9] Direct coordination of O_2 to iron results formally in an Fe(III)-superoxide, and the higher Lewis acidity of Fe(III) favors deprotonation of the monoanionic diol substrate. The semiquinone radical form of the substrate undergoes reaction with the ligated superoxide to afford an alkyl peroxo complex of Fe(II). The latter inserts an oxygen atom to give the seven-member lactone ring, which is hydrolyzed in the final step to afford the muconic semialdehyde product. Support for involvement of a semiquinone radical was provided by the use of a substrate analogue containing a cyclopropyl radical clock that underwent epimerization.[176]

Since their discovery in the 1950s, intradiol dioxygenases have been studied extensively.[163] The two most investigated of the class are catechol 1,2-dioxygenase and protocatechuate 3,4-dioxygenase. Production of intradiol dioxygenases is induced by growing different strains of soil bacteria on aromatic compounds as their sole source of carbon, which facilitated their study prior to the advent of cloning techniques. Even though intradiol cleavage is the less common route in biodegradation of aromatic molecules as compared to extradiol cleavage, the extensive investigations of intradiol dioxygenases can be attributed to the rich spectroscopy of the enzyme's iron(III) active site. The metal center supports a trigonal bipyramidal geometry with two inequivalent tyrosine ligands (axial and equatorial), two histidines, and a hydroxide (Figure 7A).

Scheme 8. Proposed Mechanism for Extradiol Catechol Dioxygenase

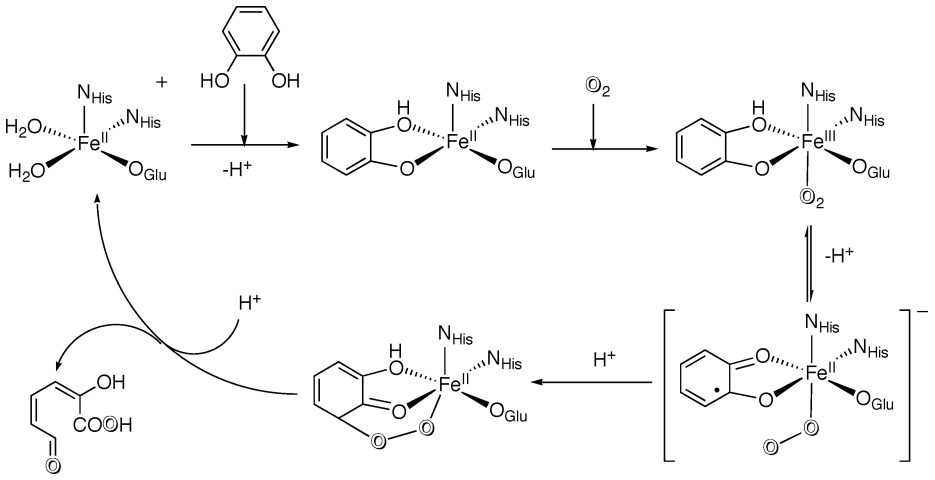

Scheme 9. Proposed Mechanism for Intradiol Dioxygenase

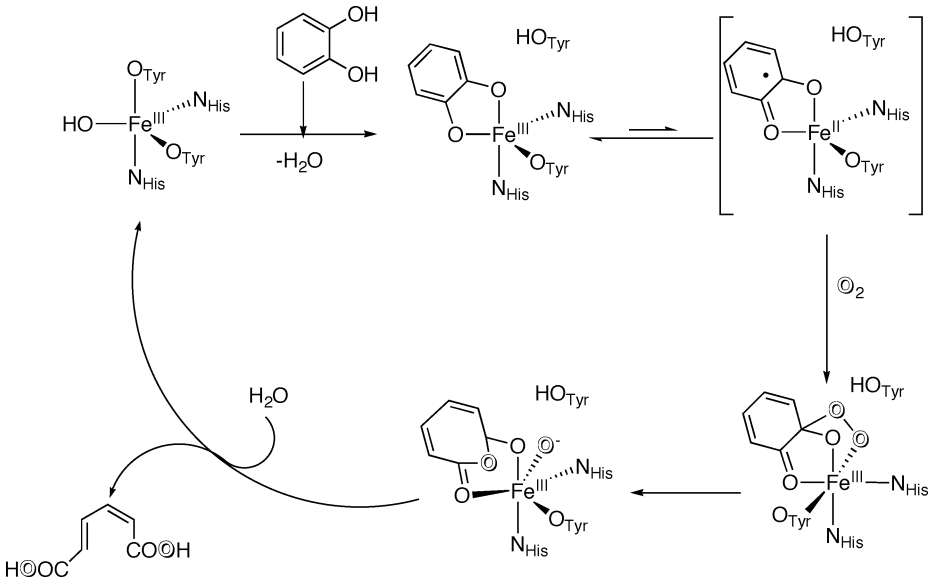

The intradiol dioxygenases, unlike their extradiol counterparts, are red-brown in color. The origin of this color is a ligand-to-metal charge transfer (LMCT) centered around ~450 nm ($\epsilon \approx 3000$ L mol^{-1} cm^{-1}), which involves the tyrosine ligands.[162] Resonance Raman spectroscopy has corroborated this assignment of the electronic transition and demonstrated two different coordination environments for the tyrosinate ligands.[176−179]

X-ray crystallographic studies on protocatechuate 3,4-dioxygenase by Ohlendorf, Lipscomb, and coworkers have revealed a wealth of information on the mode of substrate activation as well as confirmed earlier predictions from detailed spectroscopic investigations.[180−182] EPR and Mössbauer studies have indicated that the catechol substrate chelates the iron active site, which exhibits signals characteristic for high-spin Fe(III); however, the iron remains five coordinate in the ES binary complex.[183,184] The molecular structure of the enzyme substrate complex of protocatechuate 3,4-dioxygenase supported the spectroscopic interpretation. The catechol substrate donates its hydroxyl protons to the hydroxide ligand and the axial tyrosine to afford a bidentate iron(III) catecholate complex that retains the endogenous two histidine and equatorial tyrosine ligands. Due to the different trans influence of histidine and tyrosine, the Fe−$O_{catechol}$ trans to tyrosine features a bond length ~0.2 Å longer than the F−$O_{catechol}$ trans to the histidine ligand. Even though trans influence is a thermodynamic parameter and not a kinetic effect, it is believed to play an important role in the enzyme's catalysis.

The mechanism of catechol oxidation in this class of enzymes is believed to proceed via substrate activation.[182] Thus far, no evidence that is relevant to enzyme activity has been provided for iron reduction from the +3 to the +2 oxidation state. Furthermore, NO, a surrogate of O_2, does not bind the active site unless the metal is reduced by an exogenous reductant.[185] Therefore, the ketone tautomer of the coordinated substrate is attacked directly by O_2 to generate a peroxo intermediate followed by O-atom insertion into the diolate C−C bond to produce the anhydride (Scheme 9). The latter reacts with metal bound hydroxide to yield the muconic acid product, which is protonated by the previously coordinated axial tyrosine and a water molecule regenerating the catalyst.

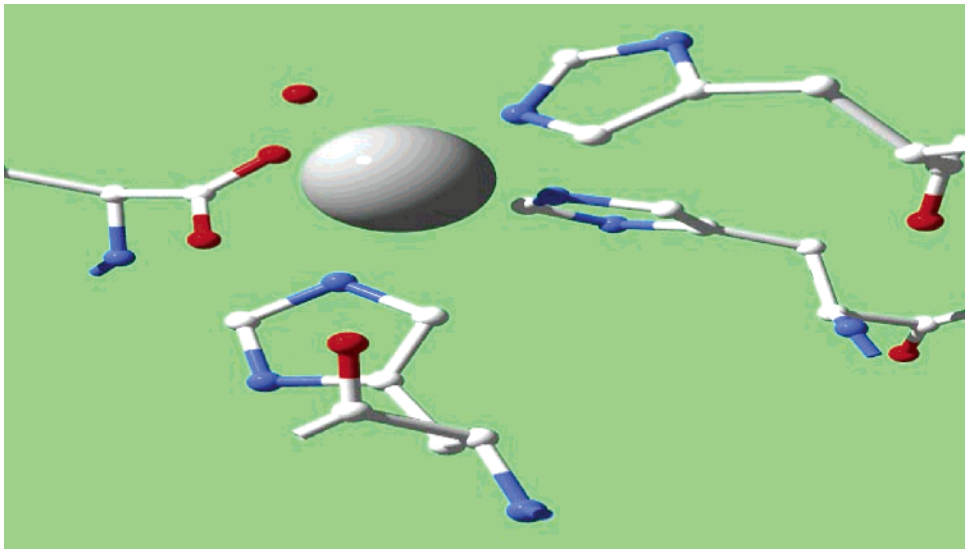

Figure 8. The non-heme iron active site of soybean lipoxygenase-3.

4.3. Lipoxygenases

Controlled hydroperoxidation of fatty acids is essential for cellular signaling, cell growth, and defense. Polyunsaturated fatty acid metabolism is regulated by cyclooxygenase and lipoxygenase.[186] Lipoxygenases (LOs) are non-heme iron dioxygenases that catalyze the hydroperoxidation of polyunsaturated fatty acids by incorporation of molecular oxygen into the 1,4-*cis*-*cis*-diene moiety of fatty acid substrates. LOs are named according to the position of peroxidation of the substrate. Unlike PAH, LOs do not catalyze a rate-determining step in a metabolic pathway. Rather, their role is to produce secondary metabolites in eicosenoid anabolism. Mammalian LOs play a significant role in the production of prostaglandins, lipoxins, and leukotrienes, which are molecules elicited during an inflammatory response.[187−192] 5-LO, 12-LO, and 15-LO are three well-characterized lipoxygenases.[193−195] Human 5-LO is involved in the synthesis of leukotrienes, which are important mediators of the inflammatory response observed in common allergies, arthritis, and asthma, through the oxidation of arachidonic acids. 12-LOs are necessary components of mitogenic responses in smooth muscle tissue and are allegedly linked to inflammatory bowel disease and psoriasis.[196,197] 15-LOs are oxidizing agents that use lipoproteins as substrates and are linked to atherosclerosis.[198] Structural investigations of lipoxygenases have revealed potential drug targets.[199] LO inhibitors are being investigated as potential anticancer drugs, and results from clinical trials seem to be encouraging.[191−193] The anabolic pathway of compounds involved in plant growth and development, such as jasmonic acid, includes LOs such as soybean L1 isozyme (SLO-1). Plant lipoxygenases generally catalyze the oxidation of linoleic acid.

X-ray single crystal structures of 1-LO, 15-LO, and 3-LO have been solved, clearly illustrating lipoxygenase as an ellipsoidal monomeric protein containing two domains.[200−204] Roughly 150 amino acids make up the N-terminal domain of LOs, which is composed of eight-stranded antiparallel β-barrel with a jellyroll topology. The catalytic domain is bigger relative to the N-terminal domain, roughly 700 amino acids, and is made up of 23 α helices and two small antiparallel β sheets. The structures also reveal a non-heme mononuclear iron site within the helical bundle of the catalytic domain. The iron atom is coordinated by three histidine ligands (His499, His504, and His690) and to the carboxylate of the final residue at the C-terminal (Ile839) in addition to an aqua ligand as well as a weak interaction with the carbonyl oxygen of the amide backbone of an asparagine (Figure 8). The rabbit enzyme differs from the soybean LOs in that it contains a fourth histidine ligand instead of the weakly bound asparagine residue.[205] There are two cavities near the active site that have been proposed to be the binding sites for molecular oxygen and substrate. Soybean 3-LO contains an additional cavity proposed to be essential for substrate discrimination.[203]

The ligand environment in LOs being histidine-rich supports high-spin iron(II) in the resting state. The estimated Fe(III)/Fe(II) reduction potential in soybean LO is 0.6 V.[206] Therefore, like the intradiol catechol dioxygenases, Fe(III) is the active form in LOs, and the enzyme enhances the rate of hydroperoxidation of the corresponding lipid via substrate activation. Substrate specificity is attributed to the region-selective hydrophobic pocket found at the catalytic domain. The as-isolated enzyme is in the Fe(II) form and is activated with the fatty acid hydroperoxide product or over a longer period of time with dioxygen.[202,207,208] Active LO features high-spin octahedral Fe(III) with a characteristic $S = {}^5/_2$ EPR signal and a charge-transfer band at 350 nm, which arises from an Fe(III) hydroxo bond.[209] Evidence for the latter has been provided by EXAFS, which featured a short Fe−O bond of 1.9 Å.[210] Upon reacting with O_2 and the fatty acid substrate, active LO forms a purple chromophore with a maximum at 585 nm and $\epsilon = 1300$ L mol^{-1} cm^{-1}. The molecular structure of this transient in soybean 3-LO showed end on

Scheme 10. Mechanism of Allylic Peroxidation Catalyzed by Lipoxygenase

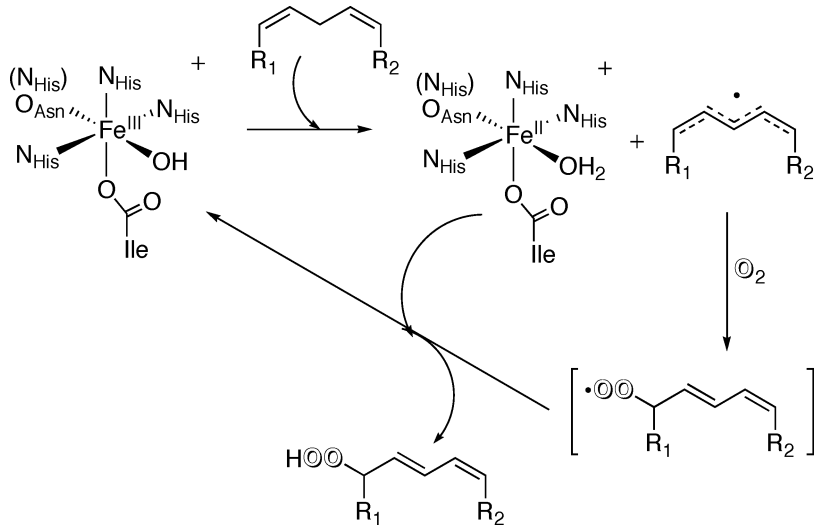

coordination of an alkyl peroxo.[211] The proposed mechanism for LO involves hydrogen abstraction from the substrate by the active Fe(III), thereby yielding a carbon centered radical intermediate. This is followed by addition of oxygen to the activated radical species, producing a peroxy radical intermediate. This second intermediate can reoxidize Fe(II) to Fe(III) (Scheme 10).[212,213] A detailed molecular explanation of the mechanism, especially during the final steps, is still being defined.[214]

5. Conclusion and Perspectives

The versatility of non-heme iron centers in biological oxidations is evident from the diversity of reactions they catalyze. Covered in this review are enzymes capable of effecting aromatic hydroxylations, C−H oxidation, desaturation, allylic peroxidation, and C−C oxidative bond cleavage. Due to advances in crystallography and cloning techniques combined with mechanistic investigations, our knowledge of non-heme iron centers has expanded tremendously over the past decade. Certain elements of simplicity in the design of mononuclear non-heme iron hydroxylases are quite apparent to the inorganic chemist and are worthy of mention. The choice of ligands, despite nature's limited pool, is astute and suited for the enzyme's targeted function. The 2-His 1-carboxylate "facial triad" motif is selected for O_2 activation, while tyrosinate (in the case of intradiol cleaving dioxygenases) and histidine (in the case of lipoxygenases) are used to favor substrate activation. The variation in ligands to favor O_2 activation versus substrate activation is illustrated in Figure 9. In addition to ligand differences, more subtle variations cannot be underestimated. One example is monodentate versus bidentate carboxylate coordination of Glu or Asp (hPAH vs cPAH and α-KG-dependent enzymes vs *cis*-dihydroxylating dioxygenases).

Even though there is beauty in simplicity, the elegance of nature's complexity cannot be overlooked. The choice and architecture of second and third coordination sphere residues in the active pocket of these enzymes play a crucial role in dictating the underlying catalytic chemistry, from mechanism to cofactor and substrate specificity. X-ray crystallography combined with mechanistic studies of site-specific mutants has and continues to unravel the biocomplexity of these enzymes. Nevertheless, many facets of the mechanisms, selectivity, and substrate specificity of non-heme iron oxygenases are not well understood. One goal of chemical researchers in this area is to understand an enzymatic reaction well enough to be able to rationally design an environmentally benign (green) molecular catalyst for the reaction. Mechanistic chemistry, therefore, forms an essential bridge between structure and function on one hand, and model systems and enzymes, on the other (Figure 10). Structural information yields

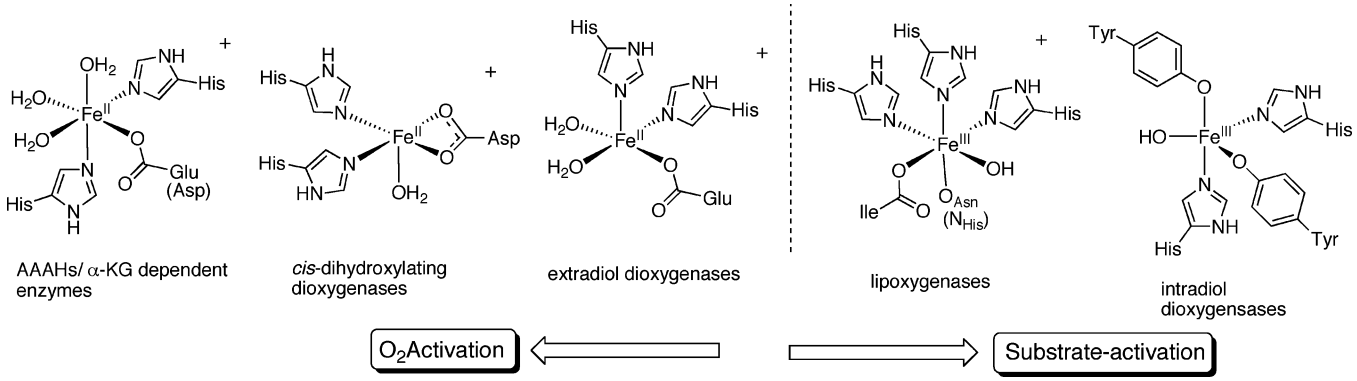

Figure 9. Active sites of non-heme iron hydroxylases showing the choice of ligands to favor O_2 versus substrate activation.

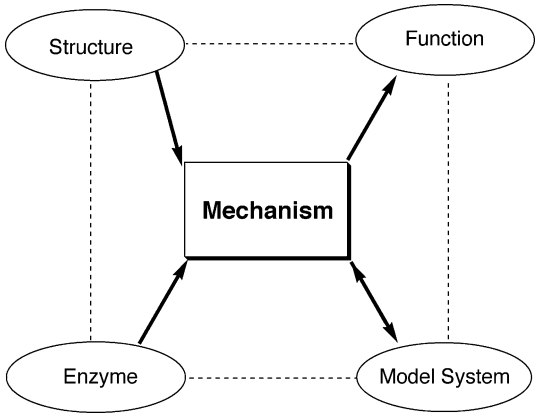

Figure 10. A diagrammatic representation of the central role mechanism plays in bridging four areas of research in enzymology.

hypotheses and predictions about function, which are validated or modified by mechanistic investigations of point mutants. Furthermore, mechanistic insights on enzymes aid in the design of functional models, which often provide mechanistic knowledge of their own that is pertinent to the real enzyme systems. Mechanistic studies of non-heme model systems were left out intentionally because they are covered by another review article in this thematic issue on Inorganic and Bioinorganic Mechanisms.[215] The significance of biomimetic studies as well as bioinspired research is not to be undervalued. An elegant example of the latter is the work of Borovik and coworkers in which second coordination sphere interactions, hydrogen bonding, are utilized to stabilize novel iron oxo (and other) structures.[216]

6. Abbreviations

AAAHs	aromatic amino acid hydroxylases
ACC	1-aminocyclopropane-1-carboxylic acid
ACCO	ACC oxidase
ADO	anthranilate-1,2-dioxygenase
AdoMet	S-adenosyl-l-methionine
AlkB	N-demethylase
AtsK	alkylsulfatase
BH_2	7,8-dihydrobiopterin
BH_4	tetrahydrobiopterin
BZDO	benzoate 1,2-dioxygenase
CaM-PK	calmodulin-dependent protein kinase
CAS	calvaminate synthase
cPAH	*Chromobacterium violaceum* phenylalanine hydroxylase
DAOCS	deacetoxycephalosporin C synthase
DHPR	dihydropteridine reductase
$DMPH_4$	6,7-dimethyltetrahydropterin
L-DOPA	3,4-dihydroxyphenylalanine
DSC	differential scanning calorimetry
DTT	dithiothreitol
FNR	ferredoxin:NADPH reductase
hPAH	human phenylalanine hydroxylase
HPP	4-hydroxyphenylpyruvate
hTPH	human tryptophan hydroxylase
α-KG	α-ketoglutarate
LMCT	ligand-to-metal charge transfer
LOs	lipoxygenases
MAP	mitogen-activated ptotein
MPH_4	6-methyltetrahydropterin
MSK1	mitogen and stress activated protein kinase 1
NDO	naphthalene 1,2-dioxygenase
oTPH	rabbit tryptophan hydroxylase
PAH	phenylalanine hydroxylase
PDO	phthalate dioxygenase
PH_4	tetrahydropterin
PKU	phenylketonuria
PRAK	p38 regulated/activated kinase
rPAH	rat phenylalanine hydroxylase
rTH	rat tyrosine hydroxylase
SLO-1	soybean L1 isozyme
SOD	superoxide dismutase
SPR	surface plasmon resonance
TAT	tyrosine amine transferase
Tau D	taurine/2-oxoglutyrate dioxygenase
TH	tyrosine hydroxylase
THA	3-(2-thienyl)-l-alanine
TPH	tryptophan hydroxylase

7. Acknowledgment

We are grateful to the NSF (grant CHE-0434637) for supporting our research in the area of non-heme iron enzymes. N.H. thanks Ms. Catherine Shields for helpful discussions.

8. References

(1) Sawyer, D. T. In *Oxygen Complexes and Oxygen Activation by Transition Metals*; Martell, A. E., Sawyer, D. T., Eds.; Plenum: New York, 1988; pp 131−148.
(2) Babcock, G. T.; Varotsis, C. J. *J. Bioenerg. Biomembr.* **1993**, *25*, 71.
(3) Khalifa, R. *Quran: The Final Testament*; Universal Unity: Fremont, 2000; p 541.
(4) Sono, M.; Roach, M. P.; Coulter, E. D.; Dawson, J. H. *Chem. Rev.* **1996**, *96*, 2841.
(5) Ferguson-Miller, S.; Babcock, G. T. *Chem. Rev.* **1996**, *96*, 2889.
(6) Nordlund, P. In *Handbook on Metalloproteins*; Bertini, I., Sigel, A., Sigel, H., Eds.; Marcel Dekker: New York, 2001; pp 461−570.
(7) Solomon, E. I.; Brunold, T. C.; Davis, M. I.; Kemsley, J. N.; Lee, S.-K.; Lehnert, N.; Neese, F.; Skulan, A. J.; Yang, Y.-S.; Zhou, J. *Chem. Rev.* **2000**, *100*, 235.
(8) Solomon, E. I.; Decker, A.; Lehnert, N. *Proc. Natl. Acad. Sci. U.S.A.* **2003**, *100*, 3589.
(9) (a) Costas, M.; Mehn, M. P.; Jensen, M. P.; Que, L., Jr. *Chem. Rev.* **2004**, *104*, 939. (b) Foster, T. L.; Caradonna, J. P. *Comprehensive coordination chemistry II*; Elsevier: New York, 2004; Vol. 8, p 343.
(10) Li, Q.-S.; Ogawa, J.; Schmid, R. D.; Shimizu, S. *Appl. Environ. Microbiol.* **2001**, *67*, 5735.
(11) (a) Kamerbeek, N. M.; Moonen, M. J. H.; Van der Ven, J. G. M.; Van Berkel, W. J. H.; Fraaije, M. W.; Janssen, D. B. *Eur. J. Biochem.* **2001**, *268*, 2547. (b) Mitchell, K. H.; Rogge, C. E.; Gierahn, T.; Fox, B. G. *Proc. Natl. Acad. Sci. U.S.A.* **2003**, *100*, 3784. (c) Leahg, J. G.; Batchelor, P. J.; Morcomb, S. M. *FEMS Microbiol. Rev.* **2003**, *27*, 449.
(12) Dix, T. A.; Ballog, G. E.; Domanico, P. L.; Benkovic, S. J. *Biochemistry* **1987**, *26*, 3354.
(13) Haavik, J.; Flatmark, T. *Eur. J. Biochem.* **1987**, *168*, 21.
(14) Moran, G. R.; Daubner, S. C.; Fitzpatrick, P. F. *J. Biol. Chem.* **1998**, *273*, 12259.
(15) Bailey, S. W.; Rebrin, I.; Boerth, S. R.; Ayling, J. E. *J. Am. Chem. Soc.* **1995**, *117*, 10203.
(16) Shiman, R. In *Folates and Pterins*, 2nd ed.; Blakley, R. L., Benkovic, S. J., Eds.; Wiley: New York, 1985; pp 179−249.
(17) Surtees, R.; Blau, N. *Eur. J. Pediatr.* **2000**, *159*, S109.
(18) Furukawa, Y. *Adv. Neurol.* **2003**, *91*, 40.
(19) Martinez, A.; Knappskog, P. M.; Haavik, J. *Curr. Med. Chem.* **2001**, *8*, 1077.
(20) (a) Powlowski, J.; Ballou, D.; Massey, V. *J. Biol. Chem.* **1989**, *264*, 16008. (b) Powlowski, J.; Ballou, D. P.; Massey, V. *J. Biol. Chem.* **1990**, *265*, 4969.
(21) Bhat, S. G.; Vaidyanathan, C. S. *Arch. Biochem. Biophys.* **1976**, *176*, 314.
(22) (a) Taguchi, H.; Armarego, W. L. F. *Med. Res. Rev.* **1998**, *18*, 43. (b) Armarego, W. L. F. *Pteridines* **1996**, *7*, 90.
(23) Kappock, T. J.; Caradonna, J. P. *Chem. Rev.* **1996**, *96*, 2659.
(24) Flatmark, T.; Stevens, R. C. *Chem. Rev.* **1999**, *99*, 2137.
(25) Fitzpatrick, P. *Annu. Rev. Biochem.* **1999**, *68*, 355.

(26) Erlandsen, H.; Stevens, R. C. *Mol. Genet. Metab.* **1999**, *68*, 103.
(27) Blau, N.; Erlandsen, H. *Mol. Genet. Metab.* **2004**, *82*, 101.
(28) Waters, P. J. *Hum. Mutat.* **2003**, *21*, 357.
(29) Erlandsen, H.; Bjorgo, E.; Flatmark, T.; Stevens, R. C. *Biochemistry* **2000**, *39*, 2208.
(30) Erlandsen, H.; Kim, J. Y.; Patch, M. G.; Han, A.; Volner, A.; Abu-Omar, M. M.; Stevens, R. C. *J. Mol. Biol.* **2002**, *320*, 645.
(31) Chen, D.; Frey, P. A. *J. Biol. Chem.* **1998**, *273*, 25594.
(32) Volner, A.; Zoidakis, J.; Abu-Omar, M. M. *J. Biol. Inorg. Chem.* **2003**, *8*, 121.
(33) Kaufman, S.; Mason, K. *J. Biol. Chem.* **1982**, *257*, 14667.
(34) Knappskog, P. M.; Flatmark, T.; Aarden, J. M.; Haavik, J.; Martinez, A. *Eur. J. Biochem.* **1996**, *242*, 813.
(35) Fusetti, F.; Erlandsen, H.; Flatmark, T.; Stevens, R. C. *J. Biol. Chem.* **1998**, *273*, 16962.
(36) Erlandsen, H.; Fusetti, F.; Martinez, A.; Hough, E.; Flatmark, T.; Stevens, R. C. *Nat. Struct. Biol.* **1997**, *4*, 995.
(37) Erlandsen, H.; Martinez, A.; Knappskog, P. M.; Haavik, J.; Hough, E.; Flatmark, T. *FEBS Lett.* **1997**, *406*, 171.
(38) Erlandsen, H.; Flatmark, T.; Stevens, R. C.; Hough, E. *Biochemistry* **1998**, *37*, 15638.
(39) Kobe, B.; Jennings, I. G.; House, C. M.; Michell, B. J.; Goodwill, K. E.; Santarsiero, B. D.; Stevens, R. C.; Cotton, R. G.; Kemp, B. E. *Nat. Struct. Biol.* **1999**, *6*, 442.
(40) Andersson, K. K.; Cox, D. D.; Que, L., Jr.; Flatmark, T.; Haavik, J. *J. Biol. Chem.* **1988**, *263*, 18621.
(41) Andersen, O. A.; Flatmark, T.; Hough, E. *J. Mol. Biol.* **2002**, *320*, 1095.
(42) Andersen, O. A.; Stokka, A. J.; Flatmark, T.; Hough, E. *J. Mol. Biol.* **2003**, *333*, 747.
(43) Wasinger, E. C.; Mitic, N.; Hedman, B.; Caradonna, J.; Solomon, E. I.; Hodgson, K. O. *Biochemistry* **2002**, *41*, 6211.
(44) Maass, A.; Scholz, J.; Moser, A. *Eur. J. Biochem.* **2003**, *270*, 1065.
(45) Dickson, P. W.; Jennings, I. G.; Cotton, R. G. *J. Biol. Chem.* **1994**, *269*, 20369.
(46) Zoidakis, J.; Sam, M.; Volner, A.; Han, A.; Vu, K.; Abu-Omar, M. M. *J. Biol. Inorg. Chem.* **2004**, *9*, 289.
(47) Teigen, K.; Froystein, N. A.; Martinez, A. *J. Mol. Biol.* **1999**, *294*, 807.
(48) Martinez, A.; Olafsdottir, S.; Flatmark, T. *Eur. J. Biochem.* **1993**, *211*, 259.
(49) Goodwill, K. E.; Sabatier, C.; Stevens, R. C. *Biochemistry* **1998**, *37*, 13437.
(50) Daubner, S. C.; Melendez, J.; Fitzpatrick, P. F. *Biochemistry* **2000**, *39*, 9652.
(51) Ellis, H. R.; Daubner, S. C.; McCulloch, R. I.; Fitzpatrick, P. F. *Biochemistry* **1999**, *38*, 10909.
(52) Daubner, S. C.; Fitzpatrick, P. F. *Biochemistry* **1999**, *38*, 4448.
(53) Jiang, G. C.; Yohrling, G. J. T.; Schmitt, J. D.; Vrana, K. E. *J. Mol. Biol.* **2000**, *302*, 1005.
(54) McKinney, J.; Teigen, K.; Froystein, N. A.; Salaun, C.; Knappskog, P. M.; Haavik, J.; Martinez, A. *Biochemistry* **2001**, *40*, 15591.
(55) Wang, L.; Erlandsen, H.; Haavik, J.; Knappskog, P. M.; Stevens, R. C. *Biochemistry* **2002**, *41*, 12569.
(56) Almas, B.; Toska, K.; Teigen, K.; Groehn, V.; Pfleiderer, W.; Martinez, A.; Flatmark, T.; Haavik, J. *Biochemistry* **2000**, *39*, 13676.
(57) Gamez, A.; Perez, B.; Ugarte, M.; Desviat, L. R. *J. Biol. Chem.* **2000**, *275*, 29737.
(58) Ellis, H. R.; Daubner, S. C.; Fitzpatrick, P. F. *Biochemistry* **2000**, *39*, 4174.
(59) Jennings, I. G.; Cotton, R. G.; Kobe, B. *Arch. Biochem. Biophys.* **2000**, *384*, 238.
(60) Jennings, I. G.; Cotton, R. G.; Kobe, B. *Eur. J. Hum. Genet.* **2000**, *8*, 683.
(61) Chehin, R.; Thorolfsson, M.; Knappskog, P. M.; Martinez, A.; Flatmark, T.; Arrondo, J. L.; Muga, A. *FEBS Lett.* **1998**, *422*, 225.
(62) Flatmark, T.; Stokka, A. J.; Berge, S. V. *Anal. Biochem.* **2001**, *294*, 95.
(63) Stokka, A. J.; Flatmark, T. *Biochem. J.* **2003**, *369*, 509.
(64) Thorolfsson, M.; Ibarra-Molero, B.; Fojan, P.; Petersen, S. B.; Sanchez-Ruiz, J. M.; Martinez, A. *Biochemistry* **2002**, *41*, 7573.
(65) Thorolfsson, M.; Teigen, K.; Martinez, A. *Biochemistry* **2003**, *42*, 3419.
(66) Yamauchi, T.; Nakata, H.; Fujisawa, H. *J. Biol. Chem.* **1981**, *256*, 5404.
(67) Atkinson, J.; Richtand, N.; Schworer, C.; Kuczenski, R.; Soderling, T. *J. Neurochem.* **1987**, *49*, 1241.
(68) Aitken, A. *Trends Cell Biol.* **1996**, *6*, 341.
(69) Kuhn, D. M.; Arthur, R., Jr.; States, J. C. *J. Neurochem.* **1997**, *68*, 2220.
(70) Ramsey, A. J.; Fitzpatrick, P. F. *Biochemistry* **1998**, *37*, 8980.
(71) Ramsey, A. J.; Fitzpatrick, P. F. *Biochemistry* **2000**, *39*, 773.
(72) Toska, K.; Kleppe, R.; Armstrong, C. G.; Morrice, N. A.; Cohen, P.; Haavik, J. *J. Neurochem.* **2002**, *83*, 775.
(73) Bobrovskaya, L.; Dunkley, P. R.; Dickson, P. W. *J. Neurochem.* **2004**, *90*, 857.
(74) McCulloch, R. I.; Daubner, S. C.; Fitzpatrick, P. F. *Biochemistry* **2001**, *40*, 7273.
(75) Miller, R. J.; Benkovic, S. J. *Biochemistry* **1988**, *27*, 3658.
(76) Bailey, S. W.; Ayling, J. E. *Biochem. Biophys. Res. Commun.* **1978**, *85*, 1614.
(77) Pike, D. C.; Hora, M. T.; Bailey, S. W.; Ayling, J. E. *Biochemistry* **1986**, *25*, 4762.
(78) Shiman, R.; Gray, D. W.; Hill, M. A. *J. Biol. Chem.* **1994**, *269*, 24637.
(79) Martinez, A.; Olafsdottir, S.; Haavik, J.; Flatmark, T. *Biochem. Biophys. Res. Commun.* **1992**, *182*, 92.
(80) Fitzpatrick, P. F. *Biochemistry* **1991**, *30*, 3658.
(81) Hamdan, F. F.; Ribeiro, P. *J. Biol. Chem.* **1999**, *274*, 21746.
(82) Xia, T.; Gray, D. W.; Shiman, R. *J. Biol. Chem.* **1994**, *269*, 24657.
(83) Kappock, T. J.; Harkins, P. C.; Friedenberg, S.; Caradonna, J. P. *J. Biol. Chem.* **1995**, *270*, 30532.
(84) Solstad, T.; Flatmark, T. *Eur. J. Biochem.* **2000**, *267*, 6302.
(85) Martinez, A.; Knappskog, P. M.; Olafsdottir, S.; Doskeland, A. P.; Eiken, H. G.; Svebak, R. M.; Bozzini, M.; Apold, J.; Flatmark, T. *Biochem. J.* **1995**, *306*, 589.
(86) Fitzpatrick, P. F. *Biochemistry* **1991**, *30*, 6386.
(87) Fitzpatrick, P. F. *Adv. Enzymol. Relat. Areas Mol. Biol.* **2000**, *74*, 235.
(88) Klinman, J. P. *J. Biol. Inorg. Chem.* **2001**, *6*, 1.
(89) Francisco, W. A.; Tian, G.; Fitzpatrick, P. F.; Klinman, J. P. *J. Am. Chem. Soc.* **1998**, *120*, 4057.
(90) Massey, V. *J. Biol. Chem.* **1994**, *269*, 22459.
(91) Moran, G. R.; Derecskei-Kovacs, A.; Hillas, P. J.; Fitzpatrick, P. F. *J. Am. Chem. Soc.* **2000**, *122*, 4535.
(92) Frantom, P. A.; Fitzpatrick, P. F. *J. Am. Chem. Soc.* **2003**, *125*, 16190.
(93) Zoidakis, J.; Lucinian, T.; Abu-Omar, M. M., personal communication.
(94) Groves, T. J. *J. Chem. Educ.* **1985**, *62*, 928.
(95) Bruice, T. C. In *Mechanistic Principles of Enzyme Activity*; Liebman, J. F., Greenberg, A., Eds.; VCH Publishers: New York, 1988; pp 227−277.
(96) Guroff, G.; Daly, J. W.; Jerina, D. M.; Renson, J.; Witkop, B.; Udenfriend, S. *Science* **1967**, *157*, 1524.
(97) Bassan, A.; Blomberg, M. R. A.; Seigbahn, P. E. M. *Chem.-Eur. J.* **2003**, *9*, 4055.
(98) Que, L., Jr. *Nat. Struct. Biol.* **2000**, *7*, 182.
(99) Fitzpatrick, P. F.; Ralph, E. C.; Ellis, H. R.; Willmon, O. J.; Daubner, S. C. *Biochemistry* **2003**, *42*, 2081.
(100) Daubner, S. C.; Fitzpatrick, P. F. *Biochemistry* **1998**, *37*, 16440.
(101) Kinzie, S. D.; Thevis, M.; Ngo, K.; Whitelegge, J.; Loo, J. A.; Abu-Omar, M. M. *J. Am. Chem. Soc.* **2003**, *125*, 4710.
(102) Liu, A.; Ho, R. Y. N.; Que, L., Jr.; Ryle, M. J.; Phinney, B. S.; Hausinger, R. P. *J. Am. Chem. Soc.* **2001**, *123*, 5126.
(103) Ryle, M. J.; Liu, A.; Muthukumaran, R. B.; Ho, R. Y. N.; Koehntop, K. D.; McCracken, J.; Que, L., Jr.; Hausinger, R. P. *Biochemistry* **2003**, *42*, 1854.
(104) Ormo, M.; deMare, F.; Regnstrom, K.; Aberg, A.; Sahlin, M.; Ling, J.; Loehr, T. M.; Sanders-Loehr, J.; Sjoberg, B.-M. *J. Biol. Chem.* **1992**, *267*, 8711.
(105) Logan, D. T.; deMare, F.; Persson, B. O.; Slaby, A.; Sjoberg, B.-M.; Nordlund, P. *Biochemistry* **1998**, *37*, 10798.
(106) Goodwill, K. E.; Sabatier, C.; Marks, C.; Raag, R.; Fitzpatrick, P. F.; Stevens, R. C. *Nat. Struct. Biol.* **1997**, *4*, 578.
(107) Daubner, S. C.; Moran, G. R.; Fitzpatrick, P. F. *Biochem. Biophys. Res. Commun.* **2002**, *292*, 639.
(108) Han, A.; Abu-Omar, M. M., personal communication.
(109) Guixé, V.; Rodriguez, P. H.; Babul, J. *Biochemistry* **1998**, *37*, 13269.
(110) Abeles, F. B.; Morgan, P. W.; Salveit, M. E., Jr. The biosynthesis of ethylene. In *Ethylene in plant biology*, 2nd ed.; Academic Press: San Diego, 1992.
(111) Hontzeas, N.; Saleh, S.; Glick, B. R. G. *Mol. Plant-Microbe Interact.* **2004**, *17*, 865.
(112) Hamilton, A. J.; Lycett, G. W.; Grierson, D. *Nature* **1990**, *346*, 284.
(113) Ververidis, P.; John, P. *Phytochemistry* **1991**, *30*, 725.
(114) Prescott, A. G.; John, P. *Annu. Rev. Plant Physiol. Plant Mol. Biol.* **1996**, *47*, 245.
(115) Gray, J.; Picton, S.; Shabbeer, J.; Schuch, W.; Grierson, D. *Plant Mol. Biol.* **1992**, *19*, 69.
(116) Woodson, W. R.; Park, K. Y.; Drory, A.; Larsen, P. B.; Wang, H. *Plant Physiol.* **1992**, *99*, 526.
(117) Spanu, P.; Reinhardt, D.; Boller, T. *EMBO J.* **1991**, *10*, 2007.
(118) Kende, H.; Zeevaart, J. *Plant Cell* **1997**, *9*, 1197.
(119) Chae, H. S.; Cho, Y. G.; Park, M. Y.; Lee, M. C.; Eun, M. Y.; Kang, B. G.; Kim W. T. *Plant Cell Physiol.* **2000**, *41*, 354.
(120) Raz, V.; Ecker, J. R. *Development* **1999**, *126*, 3661.
(121) Silk, W. H.; Erickson, R. O. *Am. J. Bot.* **1978**, *65*, 310.
(122) Ecker, J. R. *Science* **1995**, *268*, 667.
(123) Woeste, K. E.; Ye, C.; Kieber, J. J. *Plant Physiol.* **1999**, *119*, 521.

(124) Zhang, Z.; Schofield, C. J.; Baldwin, J. E.; Thomas, P.; John, P. *Biochem. J.* **1995**, *307*, 77.
(125) McGarvey, D.; Christoffersen, R. E. *J. Biol. Chem.* **1992**, *267*, 5964.
(126) McRae, D. G.; Baker, J. E.; Thompson, J. E. *Plant Cell Physiol.* **1982**, *23*, 375.
(127) Pirrung, M. C. *Acc. Chem. Res.* **1999**, *32*, 711.
(128) Apelbaum, A.; Wang, S. Y.; Burgoon, A. C.; Baker, J. E.; Lieberman, M. *Plant Physiol*. **1981**, *67*, 74.
(129) Moya-Leon, M. A.; John, P. *Phytochemistry* **1995**, *39*, 15.
(130) Brunhuber, N. M. W.; Mort, J. L.; Christoffersen, R. E.; Reich, N. O. *Biochemistry* **2000**, *39*, 10730.
(131) Thrower, J. S.; Blalock, R., III; Klinman, J. P. *Biochemistry* **2001**, *40*, 9717.
(132) Rocklin, A. M.; Tierney, D. L.; Kofman, V.; Brunhuber, N. M. W.; Hoffman, B. M.; Christoffersen, R. E.; Reich, N. O.; Lipscomb, J. D.; Que, L., Jr. *Proc. Natl. Acad. Sci. U.S.A.* **1999**, *96*, 7905.
(133) Rocklin, A. M.; Kato, K.; Liu, H.-W.; Que, L., Jr.; Lipscomb, J. D. *J. Biol. Inorg. Chem.* **2004**, *9*, 171.
(134) Zhou, J.; Rocklin, A. M.; Lipscomb, J. D.; Que, L., Jr.; Solomon, E. I. *J. Am. Chem. Soc.* **2002**, *124*, 4602.
(135) Hausinger, R. P. *Crit. Rev. Biochem. Mol. Biol.* **2004**, *39*, 21.
(136) (a) Hanauske-Abel, H. M.; Popowicz, A. M. *Curr. Med. Chem.* **2003**, *10*, 1005. (b) Hanauske-Abel, H. M.; Günzler, V. *J. Theor. Biol.* **1982**, *94*, 421.
(137) Proshlyakov, D. A.; Henshaw, T. F.; Monterosso, G. R.; Ryle, M. J.; Hausinger, R. P. *J. Am. Chem. Soc.* **2004**, *126*, 1022.
(138) (a) Riggs-Gelasco, P. J.; Price, J. C.; Guyer, R. B.; Brehn, J. H.; Barr, E. W.; Bollinger, J. M., Jr.; Krebs, C. *J. Am. Chem. Soc.* **2004**, *126*, 8108. (b) Price, J. C.; Barr, E. W.; Tirupati, B.; Bollinger, J. M., Jr.; Krebs, C. *Biochemistry* **2003**, *42*, 7497. (c) Price, J. C.; Barr, E. W.; Glass, T. E.; Krebs, C.; Bollinger, J. M., Jr. *J. Am. Chem. Soc.* **2003**, *125*, 13008.
(139) Müller, I.; Kahnert, A.; Pape, T.; Sheldrick, G. M.; Meyer-Klaucke, W.; Dierks, T.; Kertesz, M.; Usón, I. *Biocehmistry* **2004**, *43*, 3075.
(140) Valegård, K.; Terwisscha von Scheltinga, A. C.; Dubus, A.; Ranghino, G.; Öster, L. M.; Hajdu, J.; Andersson, I. *Nat. Struct. Biol.* **2004**, *11*, 95.
(141) Gibson, D. T.; Parales, R. E. *Curr. Opin. Biotechnol.* **2000**, *11*, 236.
(142) Lau, P. C. K.; De Lozenzo, V. *Environ. Sci. Biotechnol.* **1999**, 124A.
(143) Kauppi, B.; Lee, K.; Carredano, E.; Parales, R. E.; Gibson, D. T.; Eklund, H.; Ramaswamy, S. *Structure* **1998**, *6*, 571.
(144) (a) Jeffrey, A. M.; Yeh, H. J. C.; Jerina, D. M.; Patel, T. R.; Davey, J. F.; Gibson, D. T. *Biochemistry* **1975**, *14*, 575. (b) Gassner, G. T.; Ludwig, M. L.; Gatti, D. L.; Correll, C. C.; Ballou, D. P. *FASEB J.* **1995**, *9*, 1411.
(145) Resnick, S. M.; Gibson, D. T. *J. Ind. Microbiol.* **1996**, *17*, 438.
(146) Lee, K.; Gibson, D. T. *J. Bacteriol.* **1996**, *178*, 3353.
(147) Lange, C. C.; Wackett, L. P. *J. Bacteriol.* **1997**, *179*, 3858.
(148) Lee, K. *J. Bacteriol.* **1999**, *181*, 2719.
(149) Carredano, E.; Karlsson, A.; Kauppi, B.; Choudhury, D.; Parales, R. E.; Parales, J. V.; Lee, K.; Gibson, D. T.; Eklund, H.; Ramaswamy, S. *J. Mol. Biol.* **2000**, *296*, 701.
(150) Karlsson, A.; Parales, J. V.; Parales, R. E.; Gibson, D. T.; Eklund, H.; Ramaswamy, S. *Science* **2003**, *299*, 1039.
(151) Correll, C. C.; Batie, C. J.; Ballou, D. P.; Ludwig, M. L. *Science* **1992**, *258*, 1604.
(152) Karlsson, A.; Beharry, Z. M.; Eby, D. M.; Coulter, E. D.; Neidle, E. L.; Kurtz, D. M., Jr.; Eklund, H.; Ramaswarmy, S. *J. Mol. Biol.* **2002**, *318*, 261.
(153) Wolfe, M. D.; Parales, J. V.; Gibson, D. T.; Lipscomb, J. D. *J. Biol. Chem.* **2001**, *276*, 1945.
(154) Wolfe, M. D.; Lipscomb, J. D. *J. Biol. Chem.* **2001**, *278*, 829.
(155) Yang, T. C.; Wolfe, M. D.; Neibergali, M. B.; Mekmouche, Y.; Lipscomb, J. D.; Hoffman, B. M. *J. Am. Chem. Soc.* **2003**, *125*, 7056.
(156) Wolfe, M. D.; Altier, D. J.; Stubna, A.; Popescu, C. V.; Münck, E.; Lipscomb, J. D. *Biochemistry* **2002**, *41*, 9611.
(157) Parales, R. E.; Parales, J. V.; Gibson, D. T. *J. Bacteriol.* **1999**, *181*, 1831.
(158) Beharry, Z. M.; Eby, D. M.; Coulter, E. D.; Viswanathan, R.; Neidle, E. L.; Phillips, R. S.; Kurtz, D. M., Jr. *Biochemistry* **2003**, *42*, 13625.
(159) Bassan, A.; Blomberg, M. R. A.; Siegbahn, P. E. M. *J. Biol. Inorg. Chem.* **2004**, *9*, 439.
(160) Bassan, A.; Blomberg, M. R. A.; Borowski, T.; Siegbahn, P. E. M. *J. Phys. Chem. B* **2004**, *108*, 13031.
(161) Wolfe, M. D.; Lipscomb, J. D. *J. Biol. Chem.* **2003**, *278*, 829.
(162) Lipcomb, J. D.; Orville, A. M. In *Metal Ions in Biological Systems*; Sigel, H., Sigel, A., Eds.; Mercel Dekker: New York, 1992; Vol. 28, pp 243−298.
(163) Broderick, J. B. *Essays Biochem.* **1999**, *34*, 173.
(164) Que, L., Jr.; Reynolds, M. F. In *Metal Ions in Biological Systems*; Sigel, H., Sigel, A., Eds.; Mercel Dekker: New York, 2000; Vol. 37, pp 505−525.
(165) Ghosal, D.; You, I.-S.; Chatterjee, D. K.; Chakrabarty, A. M. *Science* **1985**, *228*, 135.
(166) Quensen, J. F., III; Tiedje, J. M.; Boyd, S. A. *Science* **1988**, *242*, 752.
(167) Whiting, A. K.; Boldt, Y. R.; Hendrich, M. P.; Wackett, L. P.; Que, L., Jr. *Biochemistry* **1996**, *35*, 160.
(168) Hatta, T.; Mukerjee-Dhar, G.; Damborsky, J.; Kiyohara, H.; Kimbara, K. *J. Biol. Chem.* **2003**, *278*, 21483.
(169) Sugimoto, K.; Senda, T.; Aoshima, H.; Masai, E.; Fukuda, M.; Mitsui, Y. *Structure* **1999**, *7*, 953.
(170) Vetting, M. W.; Wackett, L. P.; Que, L., Jr.; Lipscomb, J. D.; Ohlendorf, D. H. *J. Bacteriol.* **2004**, *186*, 1945.
(171) Hans, S.; Eltis, L. D.; Timmis, K. N.; Muchmore, S. W.; Bolin, J. T. *Science* **1995**, *270*, 976.
(172) Senda, T.; Sugiyama, K.; Narita, H.; Yamamoto, T.; Kimbara, K.; Fukuda, M.; Sato, M.; Yano, K.; Mitsui, Y. *J. Mol. Biol.* **1996**, *255*, 735.
(173) Vaillancourt, F. H.; Barbaso, C. J.; Spiro, T. G.; Bolin, J. T.; Blades, M. W.; Turner, R. F. B.; Eltis, L. D. *J. Am. Chem. Soc.* **2002**, *124*, 2485.
(174) Sato, N.; Uragami, Y.; Nishizaki, T.; Takahashi, Y.; Sazaki, G.; Sugimoto, K.; Nonaka, T.; Masai, E.; Fukuda, M.; Senda, T. *J. Mol. Biol.* **2002**, *321*, 621.
(175) Shu, L.; Chiou, Y.-M.; Orville, A. M.; Miller, M. A.; Lipscomb, J. D.; Que, L., Jr. *Biochemistry* **1995**, *34*, 6649.
(176) Spence, E. L.; Langley, G. J.; Bugg, T. D. H. *J. Am. Chem. Soc.* **1996**, *118*, 8336.
(177) Tatsuno, Y.; Saeki, Y. *J. Am. Chem. Soc.* **1978**, *100*, 4614.
(178) Que, L., Jr.; Epstein, R. M. *Biochemistry* **1981**, *20*, 2545.
(179) Broderick, J.; O'Halloran, T. V. *Biochemistry* **1991**, *30*, 7349.
(180) Ohlendorf, D. H.; Lipscomb, J. D.; Weber, P. C. *Nature* **1988**, *336*, 403.
(181) Orville, A. M.; Elango, N.; Lipscomb, J. D.; Ohlendorf, D. H. *Biochemistry* **1997**, *36*, 10039.
(182) Orville, A. M.; Lipscomb, J. D.; Ohlendorf, D. H. *Biochemistry* **1997**, *36*, 10052.
(183) Whittaker, J. W.; Lipscomb, J. D.; Kent, T. A.; Münck, E. *J. Biol. Chem.* **1984**, *259*, 4466.
(184) Kent, T. A.; Münck, E.; Pyrz, J. W.; Que, L., Jr. *Inorg. Chem.* **1987**, *26*, 1402.
(185) Wasinger, E. C.; Davis, M. I.; Pau, M. Y. M.; Orville, A. M.; Zaleski, J. M.; Hedman, B.; Lipscomb, J. D.; Hodgson, K. O.; Solomon, E. I. *Inorg. Chem.* **2002**, *42*, 365.
(186) Prescott, S. M. *J. Biol. Chem.* **1999**, *274*, 22901.
(187) Samuelsson, B.; Rouzer, C. A.; Matsumoto, T. *Adv. Prostaglandin, Thromboxane, Leukotriene Res.* **1987**, *17A*, 1.
(188) Rouzer, C. A.; Samuelsson, B. *Adv. Prostaglandin, Thromboxane, Leukotriene Res.* **1987**, *17A*, 60.
(189) Rouzer, C. A.; Samuelsson, B. *Adv. Enzyme Regul.* **1987**, *26*, 133.
(190) Serhan, C. N.; Wong, P. Y.; Samuelsson, B. *Prostaglandins* **1987**, *34*, 201.
(191) Samuelsson, B.; Dahlen, S. E.; Lindgren, J. A.; Rouzer, C. A.; Serhan, C. N. *Science* **1987**, *237*, 1171.
(192) Miyamoto, T.; Lindgren, J. A.; Samuelsson, B. *Biochim. Biophys. Acta* **1987**, *922*, 372.
(193) Romano, M.; Claria, J. *FASEB J.* **2003**, *17*, 1986.
(194) Kuhn, H.; Walther, M.; Kuban, R. J. *Prostaglandins Other Lipid Mediators* **2002**, *68−69*, 263.
(195) Schwarz, K.; Anton, M.; Kuhn, H. *Adv. Exp. Med. Biol.* **2002**, *507*, 55.
(196) Shannon, V. R.; Stenson, W. F.; Holtzman, M. J. *Am. J. Physiol.* **1993**, *264*, G104.
(197) Shannon, V. R.; Chanez, P.; Bousquet, J.; Holtzman, M. J. *Am. Rev. Respir. Dis.* **1993**, *147*, 1024.
(198) Steinberg, D. *J. Clin. Invest.* **1999**, *103*, 1487.
(199) Whitman, S.; Gezginci, M.; Timmermann, B. N.; Holman, T. R. *J. Med. Chem.* **2002**, *45*, 2659.
(200) Gillmor, S. A.; Villasenor, A.; Fletterick, R.; Sigal, E.; Browner, M. F. *Nat. Struct. Biol.* **1997**, *4*, 1003.
(201) Vahedi-Faridi, A.; Brault, P. A.; Shah, P.; Kim, Y. W.; Dunham, W. R.; Funk, M. O., Jr. *J. Am. Chem. Soc.* **2004**, *126*, 2006.
(202) Minor, W.; Steczko, J.; Stec, B.; Otwinowski, Z.; Bolin, J. T.; Walter, R.; Axelrod, B. *Biochemistry* **1996**, *35*, 10687−701.
(203) Skrzypczak-Jankun, E.; Amzel, L. M.; Kroa, B. A.; Funk, M. O., Jr. *Proteins* **1997**, *29*, 15.
(204) Boyington, J. C.; Gaffney, B. J.; Amzel, L. M. *Biochem. Soc. Trans.* **1993**, *21 (Pt 3)*, 744.
(205) Gilmor, S. A.; Villaseñor, A.; Fletterick, R.; Sigal, E.; Browner, M. F. *Nat. Struct. Biol.* **1997**, *4*, 1003.
(206) Nelson, M. J. *Biochemistry* **1988**, *27*, 4273.
(207) Tomchick, D.; Phan, P.; Cymborowski, M.; Minor, W.; Holman, T. R. *Biochemistry* **2001**, *40*, 7509.
(208) Ruddat, V. C.; Whitman, S.; Holman, T. R.; Bernasconi, C. F. *Biochemistry* **2003**, *42*, 4172.
(209) Holman, T. R.; Zhou, J.; Solomon, E. I. *J. Am. Chem. Soc.* **1998**, *120*, 12564.
(210) Scarrow, R. C.; Trimitsis, M. G.; Buck, C. P.; Grove, G. N.; Crowling, R. A.; Nelson, M. J. *Biochemistry* **1994**, *33*, 15023.

(211) Skrzypczak-Jankun, E.; Bross, R. A.; Carroll, R. T.; Dunham, W. R.; Funck, M. O., Jr. *J. Am. Chem. Soc.* **2001**, *123*, 10814.
(212) Knapp, M. J.; Rickert, K.; Klinman, J. P. *J. Am. Chem. Soc.* **2002**, *124*, 3865−74.
(213) Glickman, M. H.; Klinman, J. P. *Biochemistry* **1995**, *34*, 14077−92.
(214) Segraves, E. N.; Holman, T. R. *Biochemistry* **2003**, *42*, 5236.
(215) Schindler, S.; Kryatov, S.; Rybak-Akimova, E. *Chem. Rev*., submitted.
(216) MacBeth, C. E.; Gupta, R.; Mitchell-Koch, K. R.; Young, V. G.; Lushington, G. H.; Thompson, W. H.; Hendrich, M. P.; Borovik, A. S. *J. Am. Chem. Soc.* **2004**, *126*, 2556.

CR040653O